ANALYSIS AND MODELING OF GROUNDWATER SYSTEM FOR WETLAND MANAGEMENT

WITH THE EXAMPLE OF THE AAMSVEEN WETLAND IN THE NETHERLANDS

SAYEH GHASEMI BAKHTIYARI
May, 2017

SUPERVISORS:
Dr. Zoltán Vekerdy
Dr.Maciek W. Lubczynski

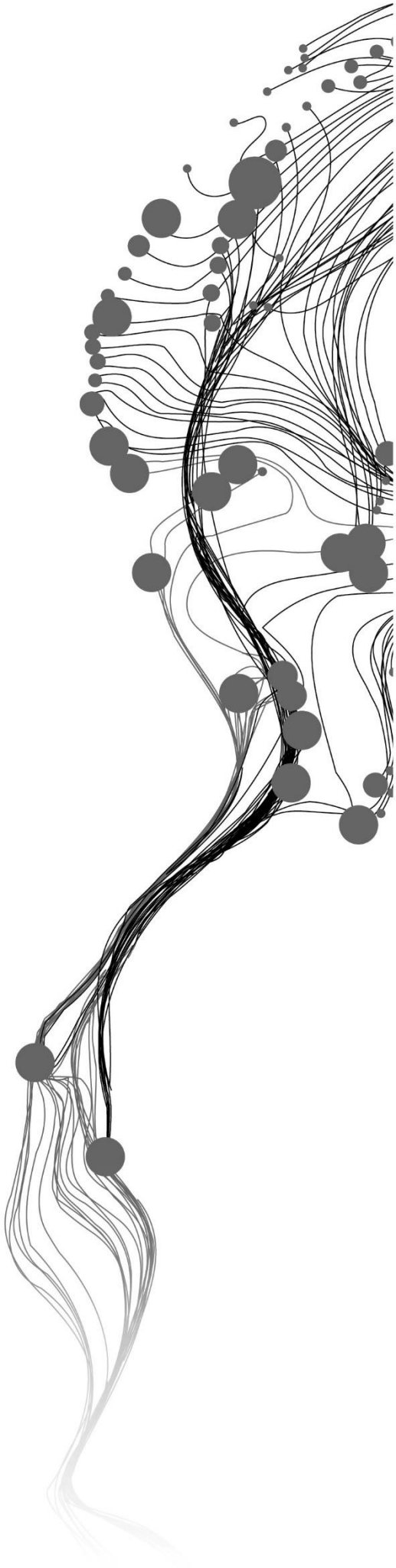

ANALYSIS AND MODELING OF GROUNDWATER SYSTEM FOR WETLAND MANAGEMENT

WITH THE EXAMPLE OF THE AAMSVEEN WETLAND IN THE NETHERLANDS

SAYEH GHASEMI BAKHTIYARI
Enschede, the Netherlands, May, 2017

Thesis submitted to the Faculty of Geo-Information Science and Earth Observation of the University of Twente in partial fulfilment of the requirements for the degree of Master of Science in Geo-information Science and Earth Observation.
Specialization: Water Resources and Environmental Management

SUPERVISORS:
Dr. Zoltán Vekerdy
Dr.Maciek W. Lubczynski

THESIS ASSESSMENT BOARD:
Dr. Suhyb Salama (Chair)
Dr. Denie Augustijn (External Examiner, University of Twente)

Dedicated to my parents,

For their endless support and

instilling me from a young age the belief that I can

ABSTRACT

Wetlands are areas in which water controls both the environment and associated biota of an area. This makes the wetlands one of the most vulnerable regions due to the anthropogenic activities. Preserving wetlands nowadays become one of the vital issues in European countries. Aamsveen wetlands located along the border of the Netherlands and Germany has been known as a Natura 2000 site. Surface water management has been done in order to preserve the wetland in 2011.

The main purpose of the modeling is the assessment of the interaction between groundwater-surface waters and to quantify the water balance of the basin for the appropriate management of the Aamsveen wetland. A steady state groundwater modeling for two main scenarios which are after and before modification has been done. MODFLOE-NWT under the ModelMuse environment was chosen to implement the wetland conceptual model. The simulation period for each scenario was five years before and after modification.

The fundamental part of the research begins with the data collection from fieldwork and analyzing in the laboratory about saturated hydraulic conductivity properties. On the other hand, using Campbell equation with the approximate soil texture fraction gives a better estimation of the area. By linking these two findings, the hydraulic conductivity values are calculated and the final zones of the conductivity were categorized. Potential evapotranspiration calculated due to the different land cover map which was created with 7 different categories. In order to take account the vegetation type and land use, the k_c was obtained from FAO-table for each vegetation. Moreover, to define the accurate driving forces, the data split into two different time periods (pre-2011 and post-2011). Because small changes in driving force could effect the results of groundwater balance since the area has a shallow groundwater.

Calibrated horizontal hydraulic conductivity values of peat layer were simulated in the range of 0.07 to 2.3 md^{-1} and for sand about 2.4 to 25 md^{-1}. The R^2 between observed and simulated head equal to 0.98 for the pos-2011 scenario set up and 0.97 for the pre-2011 scenario. Comparing water balance in both scenarios indicate that the wetland becomes wetter (33%) after the modification due to the hydraulic changes in the study area.

Key words: Aamsveen wetlands, Reconstruction, Scenario, Water balance, MODFLOW-NWT

ACKNOWLEDGEMENTS

My greatest thanks to my mother and father, for always being there giving me the opportunity to make my dreams come true.
I would like to express my deep gratitude to my first supervisor Dr. Zoltán Vekerdy for his patient guidance and advice during the thesis period. This research would not be possible without his support. I would like to also say my deep gratitude to my second supervisor Dr.Maciek Lubczynski for his valuable comments during my work.
Many thanks to Mr. Bas Worm and his other colleagues who contributed with data aquisition, from Vechtstromen, for always answered my questions regarding the study area and providing the data.
I am lucky enough to have been given the supportive gift of amazing people in my life, without all of whom, this work would not have been completed. My thanks goes to my sister Sepideh, her moral and emotional support has been invaluable and also my uncle, Khosrow Danaei, for his support and being my host for a week.
I am always grateful to my inspiring bachelor university professors Dr. Dowlati and Dr. Mehdi Zare for their encouragement and paved the way of choosing this field of study.
I am also very grateful with Murat Ucer, a research technician from ITC, for helping me during the fieldwork period.
My gratitude is also to the Erasmus Mundus programe scholarship for providing the funding which allowed me to undertake this research. Also, I would like to thank the ITC staff members of water resources and environmental management department.
Finally, I am grateful to my friends: Shoeil, Farnaz, Sara, Bani, Lukas, and Cecilia for their support in different ways during my research.

TABLE OF CONTENTS

LIST OF FIGURES

LIST OF TABLES

LIST OF ABBREVIATIONS

ArcGIS	Arc Geographic Information System
DEM	Digital Elevation Model
DINOloket	Data and Information on the Dutch subsurface
ERDAS	Earth Resource Development Assessment System
EXTDP	Extinction depth
GUI	Graphical user interface
HOB	Head Observation Package of MODFLOW
KNMI	The Royal Netherlands Metrological Institute
NAP	Normal Amsterdam Peil (equal to sea level)
NWT	Newtonian
SFR	Stream Flow Routing
MODFLOW	MODular three-dimensional finite difference groundwater FLOW model.
USGS	United States Geological Survey

1. INTRODUCTION

1.1. General background

Groundwater is one of the most significant natural resources. A great amount of groundwater has been stored and moved through aquifers in the upper portion of the Earth's crust (Kresic, 2007). In the Netherlands, annually 1700m^3 of fresh groundwater is extracted of which 60% is used for public water supply(North et al., 2007). Groundwater will be affected by other components of the water cycle such as precipitation, evapotranspiration, infiltration, run-off and this is mainly the interaction between surface water and groundwater (Naiman et al., 2013). Regarding the impacts of human activities on water balance, water management becomes vital (Brown et al., 2010). As a consequence, there is a need to quantify the relationship between external stress from human activities and water balance with models(Wang, Wang, & Anagnostou, 2007). Models are developed as tools to understand groundwater systems (Lubczynski & Gurwin, 2005). It is good to bear in mind that each model has a different level of reliability (Kinzelbach, 1986).

One of the important water body types which have been altered by humankind is wetlands. Wetlands refer to the area where water is present at the surface or near the soil for a long period of the year, especially during the growing season (Educational, 1971). The primary factor that distinguishes wetland from other water bodies is the presence of diverse flora and fauna; however, these diversities cause human to be more willing to exploit it because of the high productivity of water, fuel, and fish (Wetlands International, 2015). Climate change is one of the threats to the wetlands which is related to the changes in hydrology leading to discharges and dryness (Best et al., 1993).

This case study is about the Aamsveen wetland on the Dutch-German border. It is a former peat mining area. The Aamsveen is a bog with a surface geology consisting of eolian sand deposits of the Late Weichselian age (coversands) (Kuhry, 1985) and peat created from decomposed biomass which was formed under waterlogged conditions. This process is called paludification (Andriesse, 1988). The high organic content of top layer and the presence of peat in the wetland make the Aamsveen vulnerable to anthropogenic activities such as drainage for agriculture and peat mining (Armandine Les Landes et al., 2014). When peatlands are already drained, options for rewetting as a measure for conservation should be considered.

Wetlands have high values for ecosystem and water management purposes if the human impacts do not affect them (Malekmohammadi & Rahimi Blouchi, 2014). For this aim, European Union defines the network of nature protection areas; contain Spatial Areas of Conservation (SACs) under the Habitats Directive. This system is mainly known by the name of Natura 2000. It is vital to preserve this kind of area because human activities cause to decrease the area of peatlands across the world.

1.2. Problem statement

The Aamsveen peatland which is in the center of the study area, is surrounded by farm lands. The water has been drained due to the large scale of agriculture. Moreover, up to the middle of the twentieth century, people provided their fuel for cooking and heating from peat mining. These two major reasons made the groundwater level decrease over time. The Aamsveen presently is a Natura 2000 site to preserve the value of nature, so projects have been implemented to reconstruct the natural state of the bog by increasing primarily the groundwater level. For this aim, the surface watercourses have been changed by putting the main drain outside the wetland in 2011. After almost five years of changing the surface water course, there is a need for measuring and monitoring the hydrological process in the wetland system.

Using models enable us to simulate these processes for assessing the effects of anthropogenic impacts on the water levels. Moreover, with models, we can explore changes in conditions which would be difficult to monitor in the field. However, far too little attention has been paid so far to creating a single hydrological model for this area. The first such modeling attempt was made by Nyarugwe (2016). Although two scenarios were implemented in this work, the author failed to build one unique model. His study would have been more successful if he considered the same geology for the area and applied for the surface water courses correctly.

1.3. Research objectives

1.3.1. Main objective

Create a groundwater model that can simulate the hydrology of the Aamsveen region for wetland management purposes

1.3.2. Specific objective

- ✓ Improve the existing calibrated steady-state models of the Aamsveen catchment for 2 scenarios, each of which has 4 years of simulation period.
- ✓ Estimate the water balance of the study area in two scenarios.
- ✓ Evaluate the changes trigged by the water management interventions in 2011.

1.4. Research questions

This paper seeks to address the following questions:

- ✓ How to improve the existing steady-state model?
- ✓ What are the water balance components of the system?
- ✓ How did the changes in 2011 affect the water balance components of the Aamsveen

1.5. Research assumptions

Groundwater evapotranspiration would be negligible due to the shallow aquifer and small thick ness of unsaturated zone. (ET_u=0)

2. DESCRIPTION OF THE STUDY AREA

2.1. Study area location

The Aamsveen wetland is situated at about 5 km southeast of Enschede city on the border of the Netherlands and Germany. The central coordinate of the area is 52° 11' N, 6° 57' E. Most of the wetland located in Germany with field names Hündfelder Moor, Amtsvenn and Graeser Venn which are about 700 hectares; however, the Dutch section is about 175 ha. The area was formed during the last glacial period of wind-blown sand, covering a low-lying an ice-formed relief (Fassio, 2000). In this study, "Aamsveen" refers to the whole wetland area including both the German and the Dutch parts. The entire catchment area covers about 23 km^2 (Figure 1). Within the catchment, the area of the Aamsveen wetland is about 4 km^2.

Natura 2000 is a network of nature protection areas in the territory of the European Union. It protects about 18 percent of the vulnerable habitats such as wetlands. Protecting these areas play a crucial role in safeguard the animals and plants which need these places to survive (Natura 2000 Networking Programme, 2007). If there is any threat to the habitat types inside the Natura 2000 sites, certain human activities could be restricted or designed for the sites management and survival purpose.

Due to the environmental importance of this study area related to including the area, it is included in the list of Habitats Directives of the European Union since 1983. Nevertheless, it has undergone various changes in the past such as peat mining for fuel supply and drainage for agriculture. Landscape Overijssel has managed the Dutch section since 1967 to restore the formation of the bog (Wikipedia, 2016). Since then, some modifications were made in order to generate a self-regulating system , as summarized in Table 1(Xing, 2015):

Year	Action	Reason/purpose
1969	❖ End of peat extraction ❖ Channel dig along the lowest part of the wetland	The channel was dug to make drainage of upstream agriculture lands possible, since the altitude influence the former flow direction directly towards the Glanerbeek; this caused a lot of water logging problems for the German farmers
1983	❖ Replace the open channel with tubes	To avoid dehydration of the nature conservation area, but still drain the upstream agriculture lands through the channel replaced by tube to the Flörbach[1] and then to the Glanerbeek
1993-1995	❖ Split area into smaller compartments with dams	Raise the groundwater level by holding more rainwater and reduce the infiltration of nutrient rich waters coming from the surrounding farmlands
2005-2006	❖ Minor raises were done on the bottom level of the Glanerbeek	To reduce the amount of water that was drained from the wetland
2011	❖ Block the drain tube and reconstruct the new channel that goes around the wetland	Restore the original stream and catchment area of the Glanerbeek

Table 1: Time table of the history modification regarding the Aamsveen wetland

[1] German stream which is excluded from this research

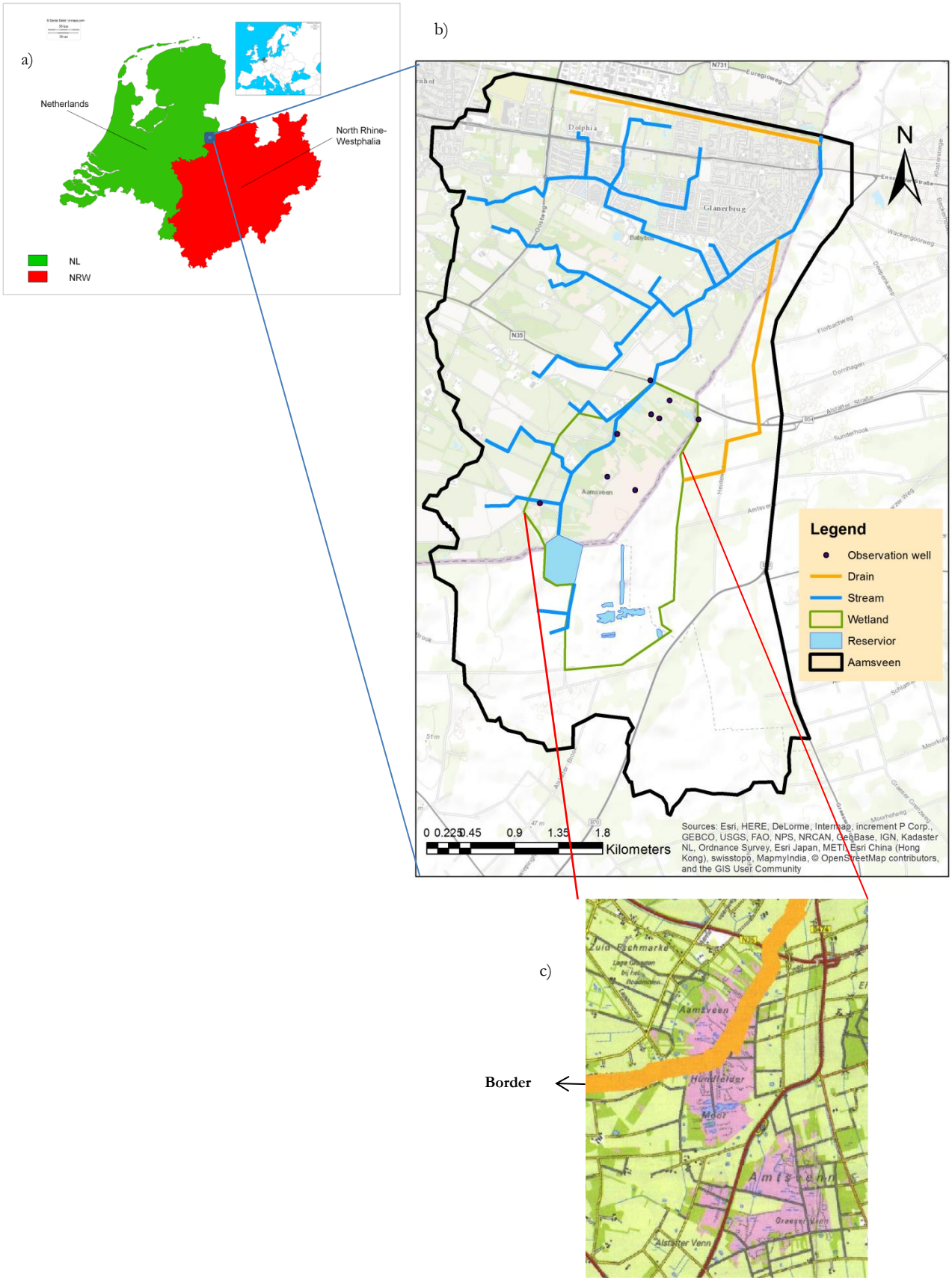

Figure 1: a) Location map of the study area catchment b) Current situation in the Aamsveen basin c) Location of the Aamsveen wetland along the Dutch-German border

2.2. Geology

The Netherlands was part of the southern North Sea Basin, during the Tertiary period. The lower middle and the upper North Sea Groups have been formed after initial calcareous deposition the Quaternary period. There is no specific source in regard this study area, so that general geology of the study area and surrounding were given in following sentences.

Due to the sea level changes and tectonics, thicknesses of lithological units affect deposition and erosion in different areas. Moreover, low sandy flat areas with exposed Pleistocene occur in the eastern and southern part of the country. Disordered blocks, push-moraine ridge, and lacustrine, eolian and fluviatile facies are the indication of glacial and interglacial periodicity. During that time, peat formed in large quantities, however, human activities over the time removed a large part of them. This accounts for substantial changes in the depositional environments and landscapes which the results can be seen now in the Netherlands (Wong et al., 2007). This phenomenon has happened in this study area as well which is shown by a red circle in Figure2.

As mentioned before, Aamsveen area with about 23km^2 located not only in the East part of the Netherlands but also include the west part of the Germany. Therefore, the geology of these two parts area is not dissimilar. The geology of Germany has been addressed in several small-scale investigations. Wong et al., (2007) claim that in the eastern part of the Netherlands, two aquifer types exist and groundwater table changes on the annual variation of the rainfall. Shallow aquifers in level areas are seasonally drained, even though, the deeper aquifers in high elevation areas are nearly without surface drainage.

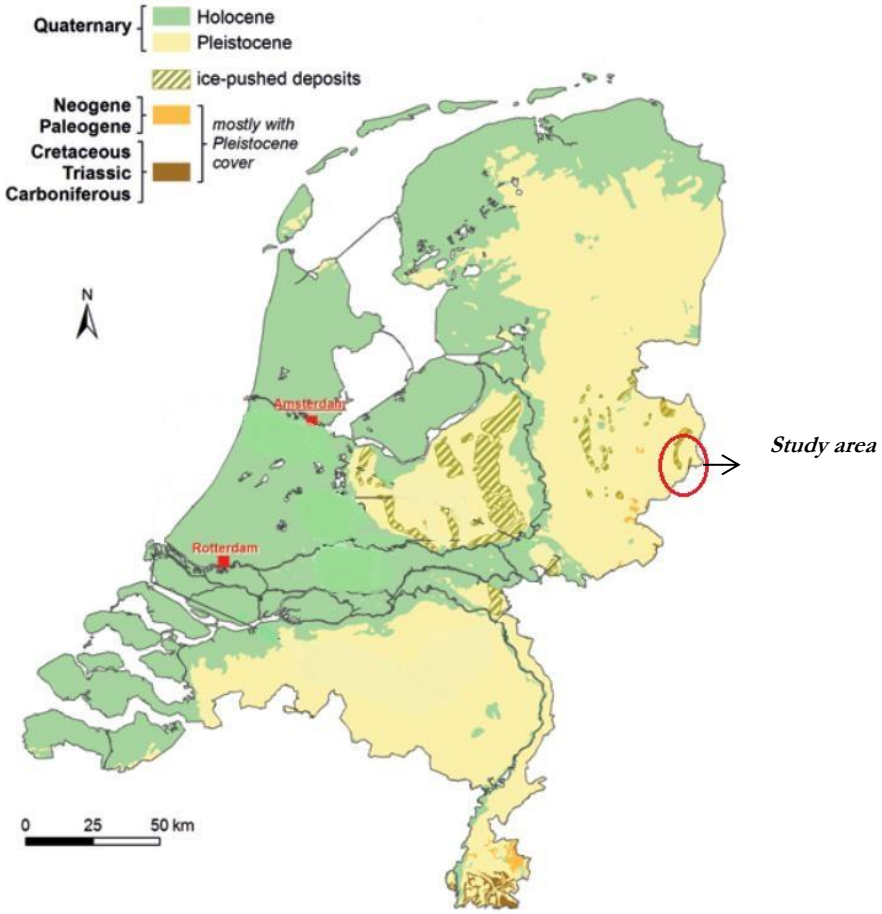

Figure 2: Geological map of the Netherlands; red circle represent the study area (source : modified from (Van Der Meulen et al., 2013))

2.3. Climate

Like most of the Netherlands, this region has oceanic climate influenced by the North Sea and the Atlantic Ocean. Due to its inland location, winters are not as mild as in the rest of the Netherlands. Royal Netherlands Metrological Institute has its online weather station in this region ("Wikipedia," 2016) which is used here to demonstrate the climatic conditions of the region (Figure 3 and Figure 4). Since the country is small there is a little variation in climate from region to region. Not to mention that the whole study area such as Germany or Netherlands part has almost the same atmosphere characteristic (Figure 3&4). Aamsveen receives an average annual rainfall about 785mm and the average daily mean temperature is 9.6° C(KNMI, 2016).

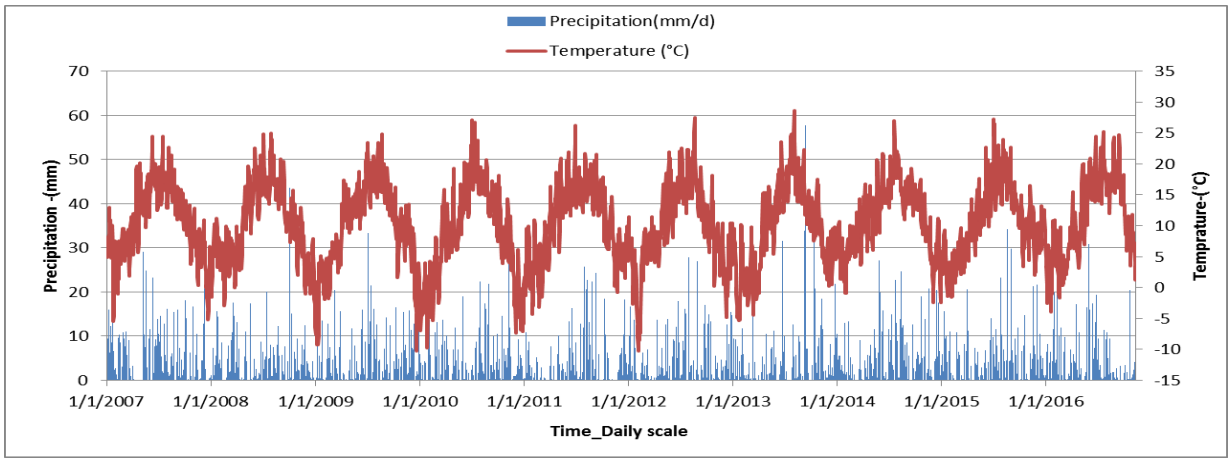

Figure 3: Daily precipitation and temperature at Twente station

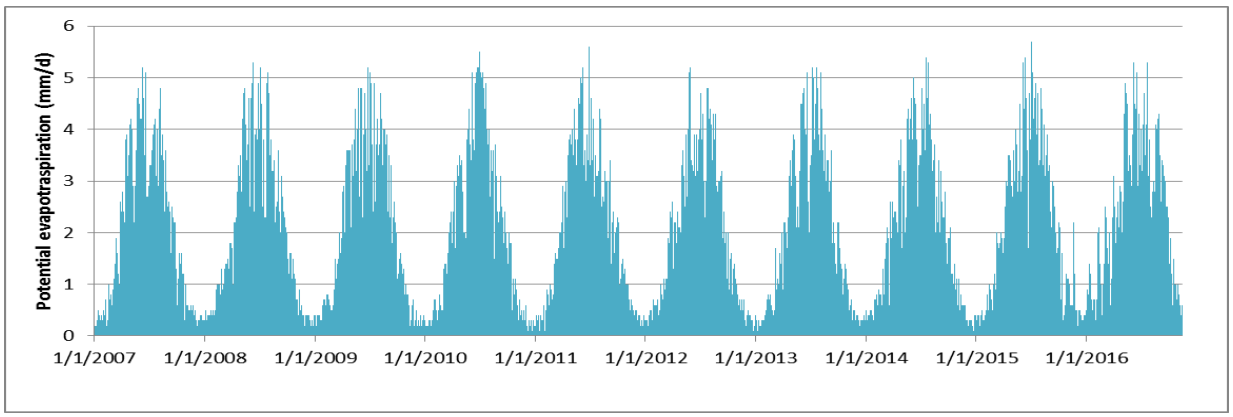

Figure 4: Daily potential evapotranspiration in Twente KNMI station.

2.4. Topography and land cover

Aamsveen is covered by a different types of vegetation such as bog, bog woodland, wet heath, Nardus grasslands and alder swamp forest (Xing, 2015). The Aamsveen peatland, located in the center of the study area, approximately coincides with the protected nature reserve area, covered by wetland (bog) vegetation (grass, bushes, wet meadows, etc.) and forests. Around the peatlands, the primary land cover is agricultural croplands and pastures. The combination of (clayey) sand and peat soil makes a considerable variation in vegetation possible, with dry and wet grassland, swamp forest and open water(Landschap Overijssel, 2007).

The study area basin is characterized by a flat topography elevation with the range of 38 to 54 meters. Figure 5 illustrates that the geo-hydrological situation correlates with topography in the west-east cross section of the Netherlands. This schematic figure has a concise explanation regarding this research study area located in Twente region (shown by rectangular). The outcrop of an impermeable hydrological base in the East of the country (red circle) coincided with the west boundary side of the study area which is outcrop of the clay and also be an impermeable layer. The groundwater level is about 42m with respect to NAP[2].

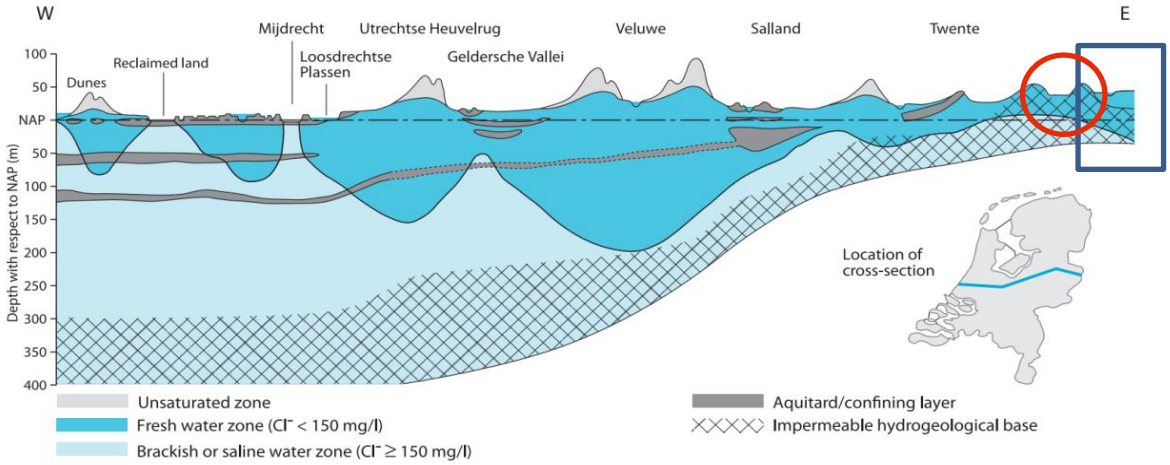

Figure 5: Schematic topographic_hydrologic west-east section showing the approximate depth of the fresh-brackish water interface (after Van de vend, 1986; source: (Dufour, 2000)

2.5. Hydrology and drainage

The Aamsveen is adjacent to the Amtsvenn in Germany in North Rhine-Westphalia province. The essence of the area is the bog in the center, combined with a landscape to a stream valley on the west side of the bog. The bog extends across the border. The peat itself had been used on a small scale dug by farmers. This caused the undulation in groundwater level in the past (Bell, J.S. & van 't Hullenaar, 2015).
A Figure 8b shows with the arrows the basin has the main water stream flowing from Southwest to Northeast direction. This stream reconstructed in the surface water modification in 2011 and starts from the weir. The weir was built for the purpose of storing some water upstream. The major stream is named Glanerbeek which has a draining effect on the groundwater inside the wetland. This is because of the stream, located in the deepest part of the region and it is cutting into the groundwater. Figure 6 is a reliable impression of hydrological issues in the Dutch section modified from (Bell, J.S. & van 't Hullenaar, 2015) and shows this situation by cross-section B-B'. The hydrological investigation in this report shows that the groundwater flow is also from south to the north part of the study area.

A great part of the transition region between the bog and Glanerbeek is also very wet during the winter (groundwater usually 0 to 20 cm below surface). This is partly due to the very thin thickness and flatness of the sand layer, whereby limited groundwater can flow to the Glanerbeek, and partly because this transition area is fed from the east, via the sand layer under the bog pits complex.

[2] NAP= Normal Amsterdam Peil=Dutch ordnance datum, approximately mean sea level

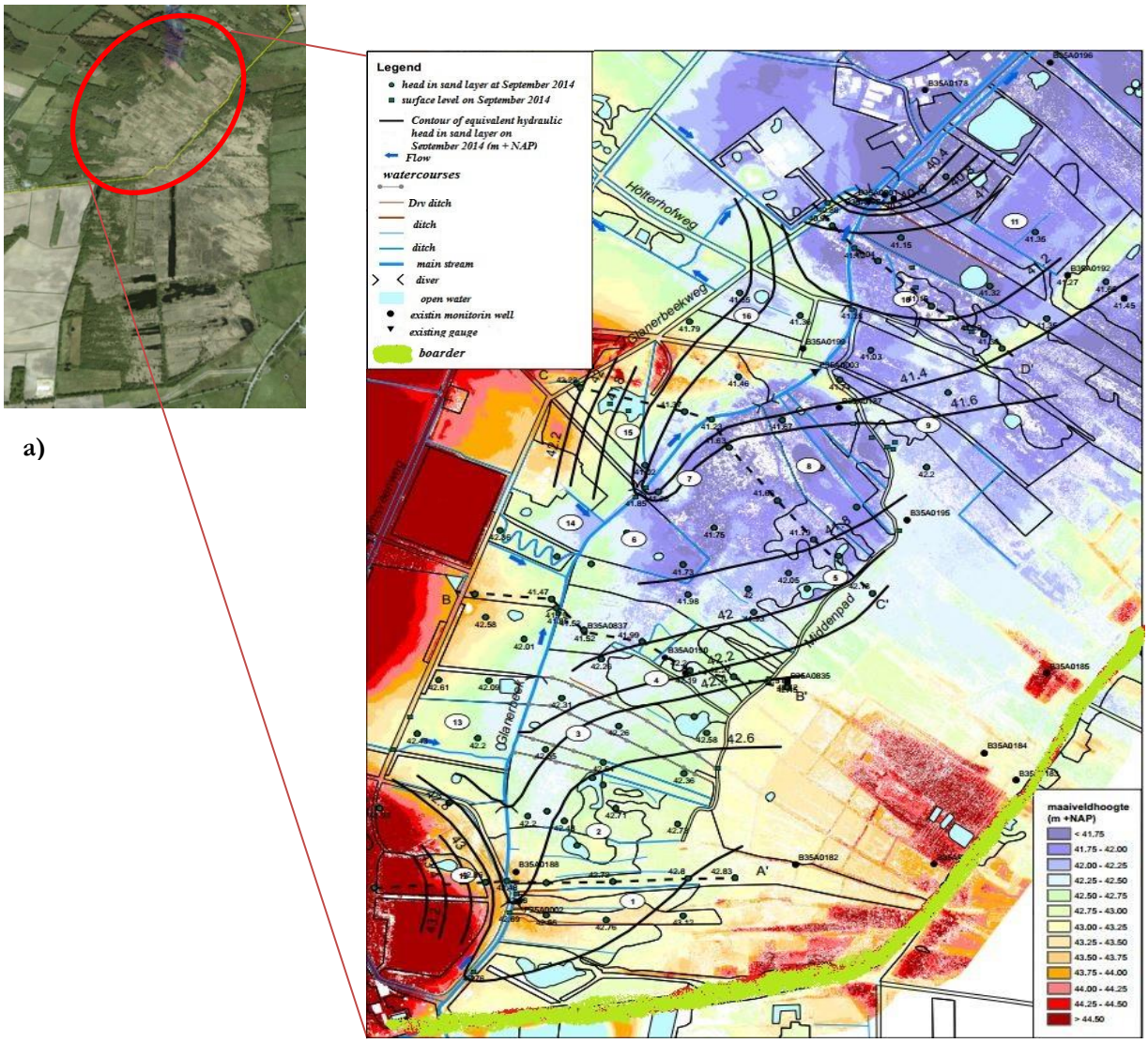

Figure 6: ***a)*** Aamsveen wetland region at the Dutch-German boarder (source: Google earth December 2009) ***b)*** Hydrological map of Dutch section (Bell, J.S. & van 't Hullenaar, 2015) ***c)*** Cross section BB' of the Aamsveen wetland showing the thickness of the layers, depth of Glanerbeek stream and water table (adopted from Nyarugwe, 2016 after (Bell, J.S. & van 't Hullenaar, 2015))

2.6. Groundwater level (potentiometric head)

The available piezometric heads obtained from the DINOloket data base (https://www.dinoloket.nl) contain mostly two logged data per month. Piezometers are used as observation points in the wetland in order to know the groundwater head. In this study area, 25 piezometers are available which are mostly inside or surrounding the Aamsveen wetland (see Appendix.1) whereas 9 piezometers were selected based on the distribution and the distance from each other and more importantly other piezometers have the limited data availability. There is also one piezometer in German side (close to the border).

2.7. Scenario's description

This research mainly focuses on the modeling of two scenarios with different surface water networks. This needs to consideration of the interaction between the groundwater and surface water. The direct relationship between surface water and groundwater management, especially in the lowlands, enable us to state the groundwater management very often means surface water management (Pellenbarg, 1989). Therefore, with the objective of increasing groundwater levels, the Water Board has changed the layout of the surface water network, as well as has built a little reservoir in the region in 2011.

In the Netherlands, Water Board is a typical Dutch institution which was founded in the 12th century. This historical old institution manages the water system or systems of the hydrological units. The hydrological unit is mostly a catchment area or a part of a catchment area. In this study area, Waterschap Vechstromen is responsible for the water management in the Overijssel province. Several modifications have been done by detail monitoring in surface water management in order to keep the wetland area secure (Table 1).

To assess the changes in the wetland water regime, two scenarios have been defined before and after the 2011 surface modification. In the pre-2011 scenario, there was a tube in which the water has been routed through the Aamsveen wetland. Unfortunately, this tube has been broken, so it functioned as a (subsurface) drain, tapping the water of the wetland. There is another drain channel in the North of the study area along with railway in both scenarios. In 2011, some parts of the drain including the wetland tube have been removed and the water has been diverted through the gauging wire into the old stream bed of the Glanerbeek, in order to restore the water course to the original stream. This modification marks the beginning of the second scenario (post-2011). The gauging wire was used for measuring the discharges from the new reservoir that has been made after 2011. The reservoir located at the upstream of the Glanerbeek stream.

The previous study of Nyarugwe(2016) in this area did not consider the model layer such as a stream or drains properly, so in this study, an improved layout is used. Figure 7 the pictorial maps show the surface water layout of the pre-2011 and post-2011 scenarios used in the current research.

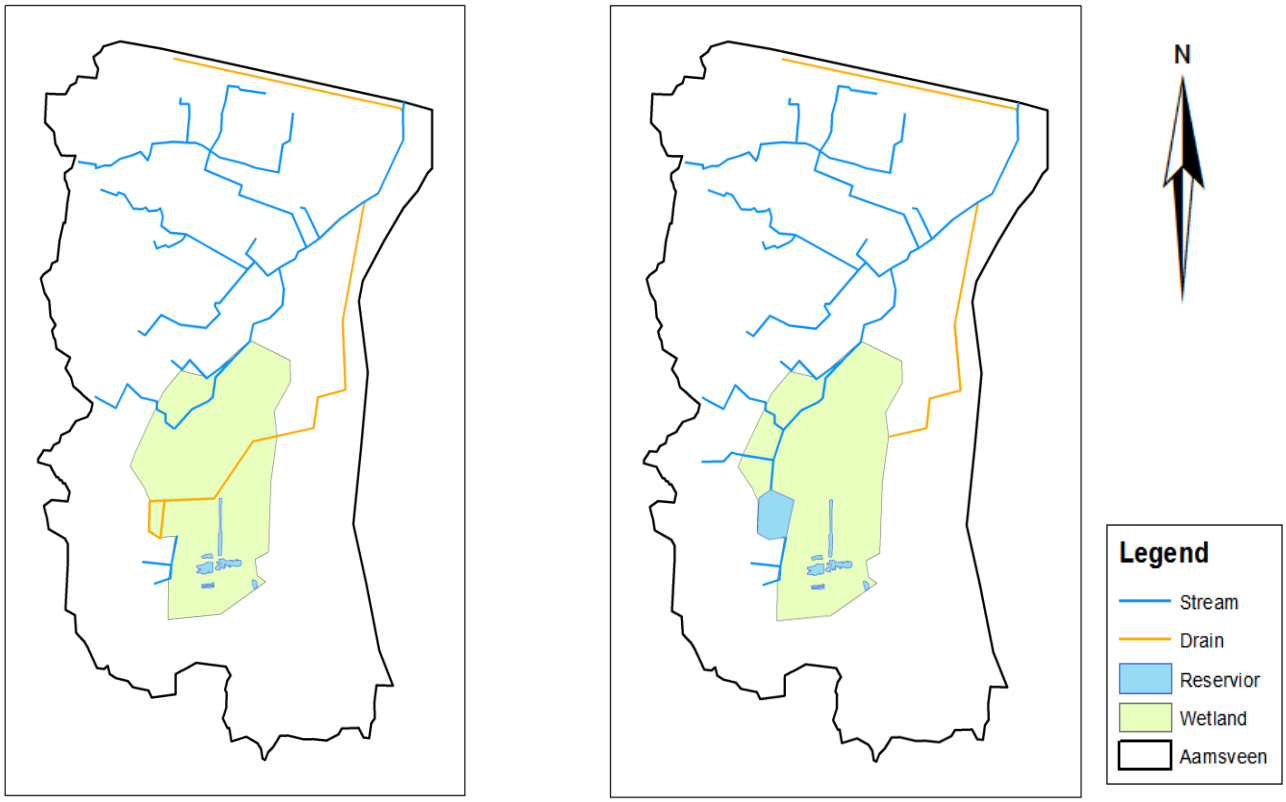

A) First scenario before

B) Second scenario after 2011

Figure 7: Pictorial implementation of two scenarios in order to restore the Aamsveen wetland A) Indicate former situation including the drain tube along the border B) Recent situation includes the reservoir and new reaches of streams (with a removed drain/tube inside the wetland).

3. RESEARCH METHODS AND MATERIALS

3.1. Methodology flowchart

In figure 8, the summary of the methodology is described. The procedure starts with data collection through fieldwork, literature review, working with the previous model, and collecting the meteorological and hydrological data. Based on the available data, a conceptual model has been defined. Finally, the parameters of the numerical model had been defined and then, based on the calibration targets, the model had been calibrated. The last step was the evaluation of the results. To define how much the model is on the accurate definition of the parameters, a sensitivity analysis was carried out.

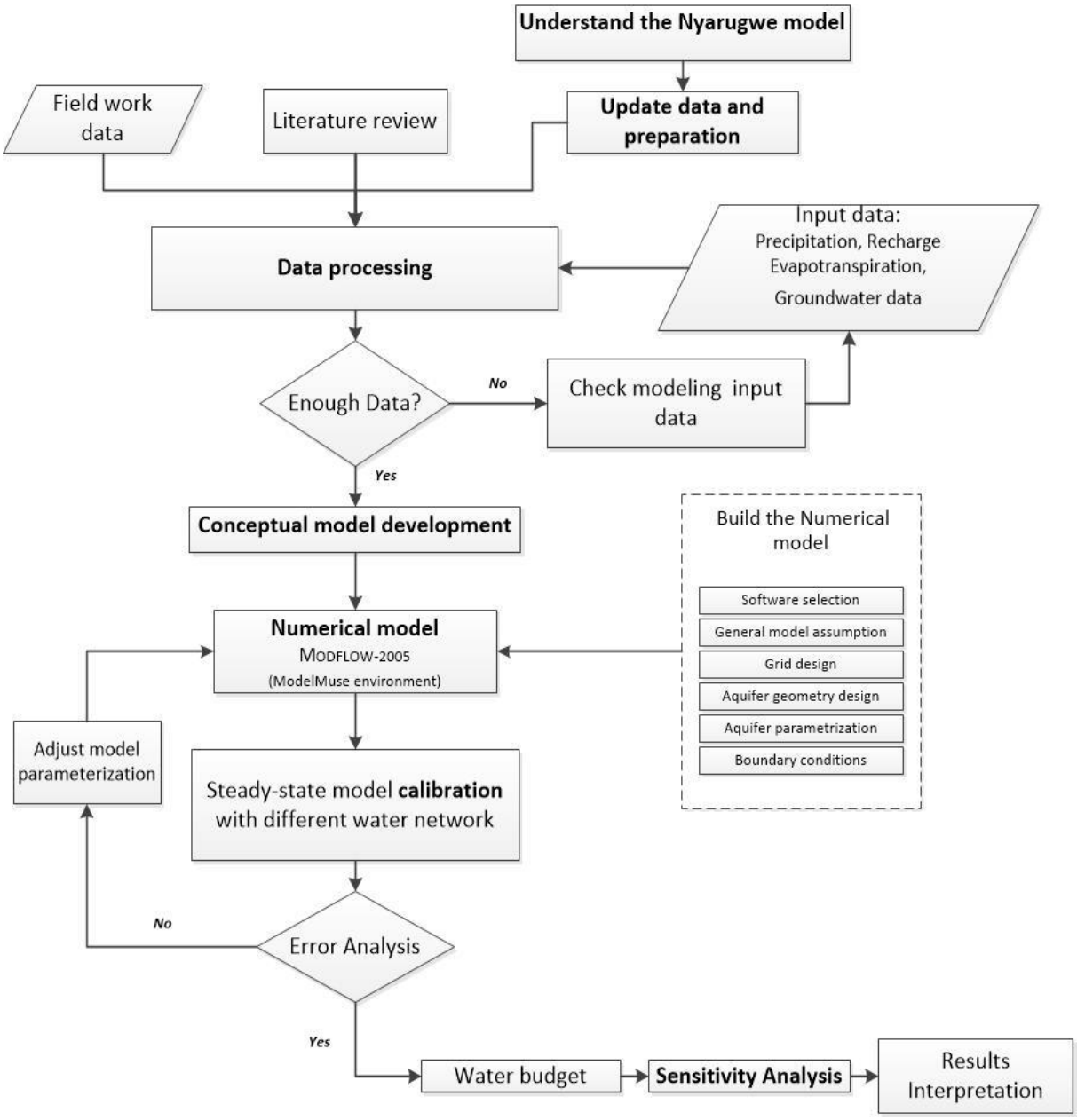

Figure 8: Research methodology flowchart

3.2. Recent studies in the Aamsveen wetland

3.2.1. Original regional model (iMod)

A regional groundwater modeling was carried out at a large scale, including this area, by the Water Board in the Netherlands. As mentioned in the previous chapter, the Water Board Vechtstromen is responsible for water management in the province of Overijssel. This regional model set up has carried out in the iMod environment of MODFLOW. The developed steady state model contains in total seven layers; however, peat which is an important phenomenon in the current research was not considered as a separate layer. First layer of regional model represent the boulder clay without considering the thin layer of sand similarly.

The spatial resolution of the model is 25*25 m. With this in mind, the level of detail concerning the hydrogeology of the Aamsveen area is not detailed enough since it is not describing the surface hydrology in Aamsveen. Figure 9outlines the digital elevation model area of the regional model in comparison with the research area. To follow hydrological boundaries the model is extended to Germany. Two stream catchments that shown in this figure confirm the boundary of the study area.

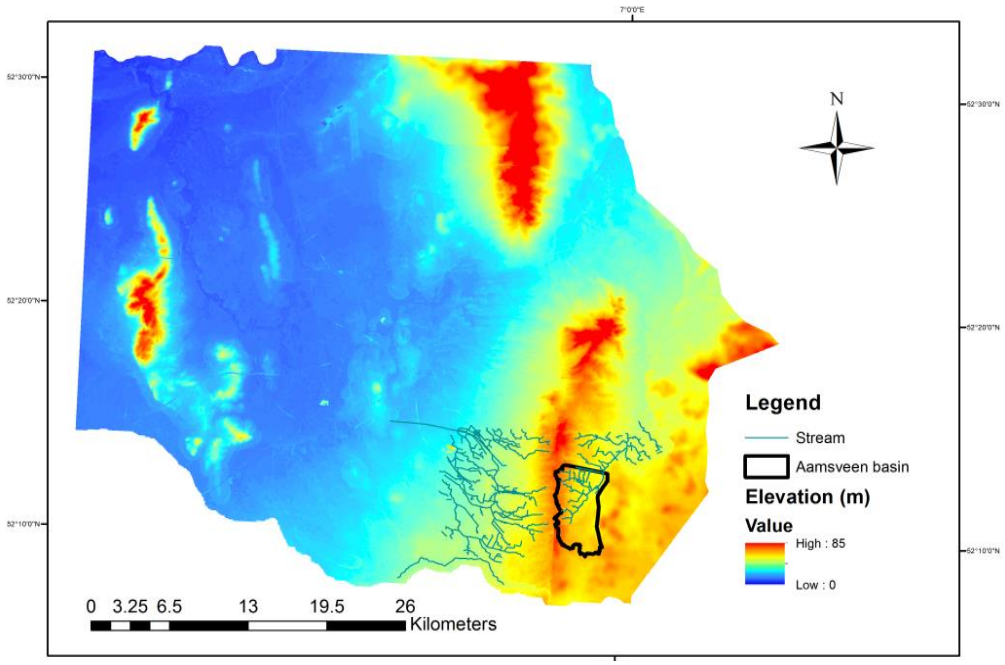

Figure 9: Digital elevation of the regional model and the current study area

3.2.2. NDVI

A study by (Xing, 2015) was conducted to monitor the changes in vegetation cover and their characteristics over years (2002-2014) in the Aamsveen wetland. These various changes in the vegetation are both natural and anthropogenic. The author also considered the areas close to the wetland in which the agricultural activities have been reduced in the last years. The result based on comparing the value of NDVI in 2004 and 2014 (figure 10), showed that the vegetation remarkably increased and the wetland became greener. The second peak of the high value in NDVI proves this fact (red box in the figure10)

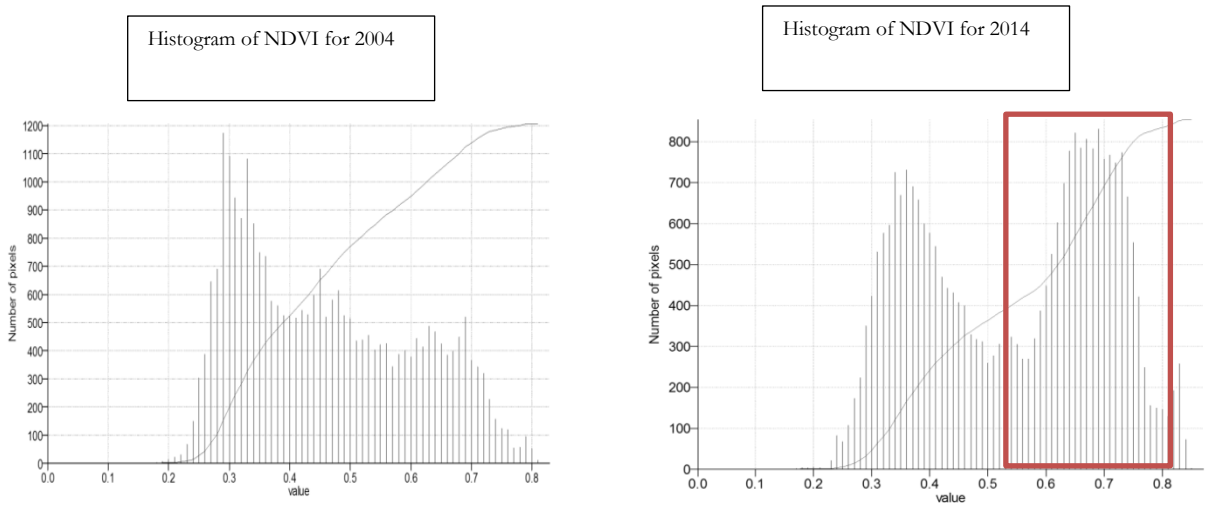

Figure 10: Comparison between the value of NDVI in 2004 and 2014 (Xing, 2015)

3.2.3. Groundwater level

Xing (2015) also conducted research about the changes of the groundwater levels in the last 20 years by mapping groundwater surface with the global polynomial interpolation (GPI) method. Based on the seasonality (wet and dry) assumption for groundwater heads, the results show that there were no significant changes in the groundwater levels neither in the dry and nor in the wet season. Xing (2015) also analyze the spatial pattern of the Aamsveen hydrology. This analysis indicates that the groundwater level is lower around the streams than at the old channel in a dry season. In the wet season, there were no spatial differences in groundwater level.

3.2.4. Steady-state groundwater model of Nyarugwe

A study has been done by Nyarugwe (2016) to simulate the effect of surface water management measures on this wetland. Two steady-state situations were modelled: one before and another after the surface water regime modification in 2011. The author concludes the wetland is becoming wetter after reconstruction as the groundwater balance in the post-2011 has more water than in the pre-2011 case. Although he got a good result in this study, he considers two independent models because the separate calibrations of the models, resulting in two different sets of hydraulic conductivities in the same area.

The Nyarugwe (2015) method suffers from some serious weaknesses. The main weakness of the study is the consideration of two slightly differing sets of geological (soil) parameters for the same region. The findings might have been much more persuasive if the author had found the real situation in the study area. For instance, hydraulic conductivity zones did not reflect soil properties of the area, and those were estimated from a small number of in situ measurements. Besides, potential evapotranspiration dealt with only two categories of land cover, that is an over simplification.

Although research has been carried out on groundwater modeling of the Aamsveen, no single study exists which adequately covers the hydrological changes in the wetland in the last years. This made it necessary to carry out the present research.

3.3. Data acquisition and model inputs preparation

According to the model requirements, geological, meteorological and hydrological data were congregated to prepare the model inputs for the post-2011 situation. Fieldwork measurements were used to define and validate the hydraulic conductivities and discharges. These are the main step before calibration procedure to deliver a compelling model simulation. In the calibration, the model parameterization was based on the mean values of the four years period of 2011-2016. The available metrological and hydrological data are shown in Table 2. In this study area, there is only one metrological station, named Twente. The data for this was obtained from the website (http://www.knmi.nl). Most of the subsurface data was acquired from the portal of the Geological Survey of the Netherlands, from the website DINO-loket (https://www.dinoloket.nl).

Data type	Quantity	Temporal / spatial resolution	Source
Hydrological data			
Groundwater level	25	Twice a month(1991-2016)	DINOloket
Gauge data (discharge)	1	(1991-2016)	DINOloket
Hydraulic conductivity	20 samples (9 points)	Calculated	Field work/Laboratory
Stream discharge	1 gauges(upstream)	Hourly(2012-2016)	Vechtstromen
Metrological data			
Precipitation	1(Twente station)	Daily (1990-2016)	KNMI
Potential evapotranspiration	1(Twente station)	Daily (1990-2016)	KNMI
Maps			
DEM (Top layer)	1	30M	Obtained from regional model
Water level map	1		Water board
Soil map	1		Soil GRID data website/ Vechtstromen
Watercourse (stream-drain)	1		Vechtstromen
Geologic map	1		Literature/ Vechtstromen

Table 2: Data availability

3.3.1. Pre-fieldwork activities

At the beginning of this study, reviewing of the literature was carried out. Moreover, the study area has been visited for several times to have a better vision and understanding of the system. Furthermore, some locations were selected for carrying out the fieldwork, since the previous model was built on lots of

simplifications in water management system, which had to be improved. This includes some of the soil properties and applying the reliable value of hydraulic conductivities based on the soil map.
The primary input data for the groundwater model was extracted from different sources such as websites academic papers, etc. The main data was piezometric heads, the regional model in iMod inputs, and the meteorological data. In order to improve the hydraulic conductivity, one of the primary plans of the field work is to collect soil map data and analyses the results in laboratory.

3.3.2. Fieldwork

One of the important factors to consider is the hydraulic conductivity of the soil over the study area. With this in mind, finding the appropriate approach to measuring this parameter becomes important. In this study, soil sampling and auger was used then the samples were analyzed in the laboratory. As the water levels in the study were very high, the sampling depth was about up to 70 cm. Nine points have been selected to acquire the soil samples including the peat or sand areas on the Dutch side of the border. Due to practical limitations, there was no possibility to have samples from the German side. The samples distribution and the measured value have shown in Appendix 2. The collections of these samples have been done by using the stainless steel rings by the size of 56*60mm.

Undisturbed method for acquire the sample helps to keep the same geology and compactness of the soil. The favourable results of soil test depend on a good sample(Simmons, Deatric, & Levis, 2014). To consider vertical hydraulic conductivity of the soil, samples were collected perpendicular to the surface. In reality, the groundwater flow has a very strong component parallel to the surface. As a result, there is a need to obtain some horizontal samples to calculate the ratio between K_h and K_v for the model as an input.
For the sake of horizontal soil sampling a soil sampling pit was dig with an area of 40*100 cm² and the same depth as of the vertical sample in the same point. Figure11 shows one of the sampling points, with the scheme of the sampling method, a photo of implementation and the tools used in the fieldwork. This method was applied for 3 points out of the total 9 locations. At the rest, only vertical sampling was carried out.

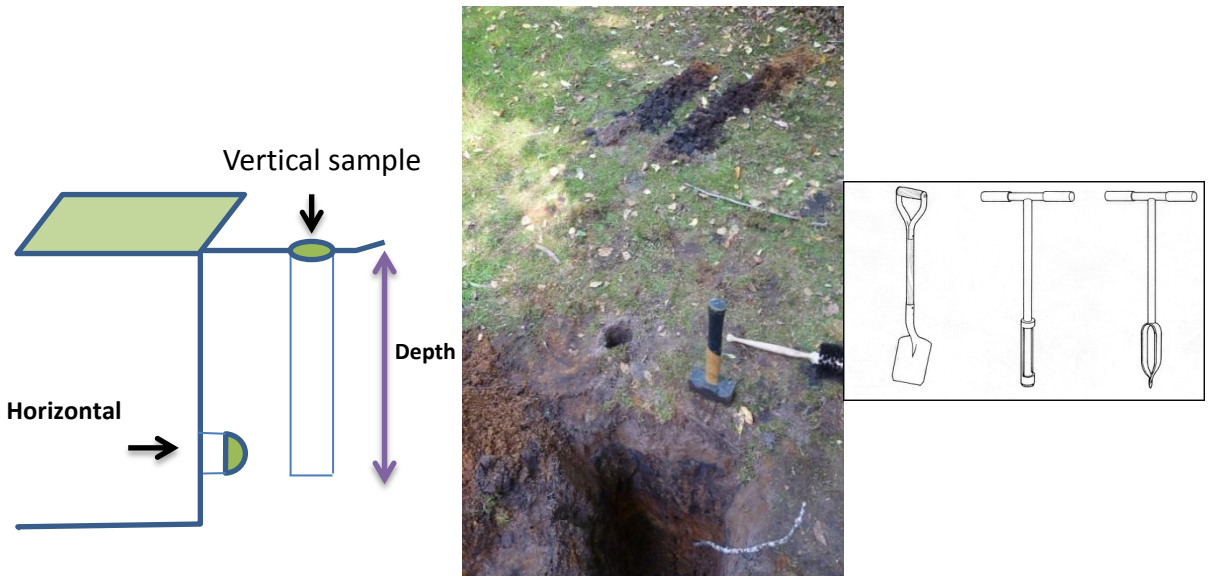

Figure 11: Some of the field work instruments for soil sampling, field work on vertical and horizontal soil sampling, schematic of the approach (From right to left)

3.3.3. Post-field work

After the field work, the collected undisturbed soil samples were tested to measure the hydraulic conductivity. In the laboratory, the samples were put in a water tank until they became saturated. Later, the samples were located in the Permeameter which is a laboratory tool to measure the saturated permeability of the soil samples. The term 'permeability' is known as the capacity of the soil to drain off water and the function of that is similar to the hydraulic conductivity definition. The permeability coefficient (K factor) was measured using the constant head testing method (Equation 1). The constant head method is the most common method to measure the K factor for the highly permeable and moderately permeable soil samples (Figure12). During the experiment the parameter's volume was measured in the burette (flow through the syphon) and the duration of the experiment was determined. Moe explanation on laboratory method is given in Appendix 3. The ratio between K_v and K_h was calculated 1/3. However, because the peat layer has a thin thickness this valued assume to be same.

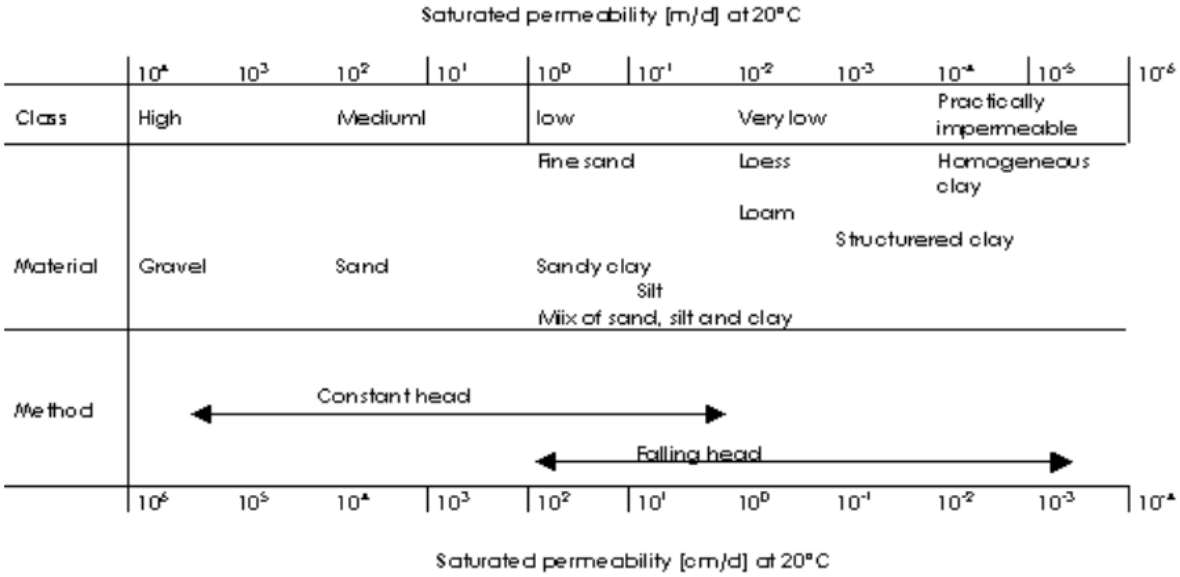

Figure 12: Schematic graph to select a method to determine the saturated permeability[md^{-1}]

$$V = K * i * A * t \rightarrow \quad K = \frac{V.L}{A.t.h} \qquad [1]$$

Where K-is the permeability coefficient or "K-factor" [cmd^{-1}]; V-is the volume of water flowing through the sample [cm^3]; L- is the length of the soil sample [cm]; A- is the cross-section surface of the sample[cm^2]; t-is the time used for flow through of water volume V [d]; h- is the water level difference between the inside and outside ring holder or sample cylinder [cm].

Even though the accuracy of this instrument is quite good, the measured values will always somewhat deviate from field conditions. This might be caused by spatial variability of samples or inaccuracies in collecting the data. Nevertheless, the difference between the laboratory measurement results and field conditions is not of many folds. Comparing the results with the soil map of the study area in the further steps showed that the field work results coincide with the corresponding values downloaded from the national soil database. Since the area includes both Dutch and German territory, there is no integrated soil map available. In this regard, a new soil map has been created which is compatible with the grid cell size of the soil map from https://www.soilgrids.org .

3.3.4. Precipitation

One of the first essential forcing data in a hydrological model is precipitation. Rain and snowmelt at land surface are partitioned into runoff, infiltration, evapotranspiration, unsaturated-zone storage, and recharge (Niswonger et al., 2006). Precipitation is an input of the recharge package that calculates infiltration can be calculated. Twente station is the closest weather station to the Aamsveen region. The data of precipitation has been acquired from there by KNMI on daily basis. The Recharge Package uses precipitation data as an input in MODFLOW. Uniform precipitation value was applied over the whole area due to the relatively small size of the wetland. The average rainfall over the simulation period in this region was calculated as for each scenario (Table 3).

	Pre-2011 (2007-2001)	**Post-2011 (2012-2016)**
Average Precipitation (md^{-1})	0.02159	0.02069

Table 3: Average precipitation value in each scenario [md^{-1}]

3.3.5. Potential evapotranspiration

Another major component of the hydrologic system is evapotranspiration. To have the daily potential evapotranspiration, the data from the metrological station is needed. Here, the raw daily potential evapotranspiration data was acquired from KNMI (Figure 4) based on the Makkink equation. Scientific community recommends to apply FAO Penman-Monteith approach to have accurate results(Wang et al., 2012), but this is a data demanding method. Makkink is a radiation based derivation of the Penman-Monteith equation(Allen, Pereira, Raes, Smith, & Ab, 1998). The derivation made from Equation 2 (Hiemstra & Sluiter, 2011).

$$\lambda ET = \frac{\Delta(R_n - G) + \rho_a . c_p . \frac{e_s - e_a}{r_a}}{\Delta + \gamma(1 + \frac{r_s}{r_a})} \qquad [2]$$

λET = latent heat flux stands for evapotranspiration
R_n= Net radiation
G= the ground heat flux
$e_s - e_a$= air vapor pressure deficit
ρ_a= air density under the constant pressure
c_p=specific heat capacity of air
Δ =Slope of the saturated vapor pressure
γ=psychometric constant
r_s, r_a = Aerodynamic and surface resistance

Instead of the whole radiation balance, Makkink potential evapotranspiration equations (Equation 3&4) use solar radiation only and simplified radiation based on FAO Penman-Monteith equation (Xu & Singh, 2002). Makkink equation is simple form of the Priestley_Taylor equation.

$$PET = c_1 \frac{\Delta}{\Delta + \gamma}(\frac{R_s}{\lambda}) - c_2 \qquad [3]$$

$$PET = 0.7 \frac{\Delta}{\Delta + \gamma}(\frac{R_s}{\lambda}) \qquad [4]$$

PET= potential evapotranspiration after Makkink
Δ = slope of the saturation vapor pressure curve

γ=psychometric constant
R_s= Solar radiation
λ = Specific (or latent) heat of evaporation
c1, c2 =Makkink coefficients (0.61, -0.12), to be calibrated to the specific site

McMahon, et al, (2013) points out that potential evapotranspiration [PET] refers to the entire covered area with growing vegetation homogeneously. ET_a in this study area was calculated by the Evapotranspiration package of MODFLOW according to the groundwater depth. Moreover, K_c factor is a crop coefficient and since K_c changes in time, it can be specific in time too. In the following more explanation about calculating the PET is presented.
There are many possible ways of defining one parameter based on the available data. In the previous study, analyze the potential evapotranspiration have not treated in much detail. However, this research, try to attach the land cover of the area to the rate of evapotranspiration which gives coherence and intelligibility to them. In this sense, the specific assumption has been considered based on the land cover map.
Evapotranspiration has been given different values based on the various land cover. A generally accepted definition of reference evapotranspiration is evaporation plus transpiration from short, well-watered grass or open water. With regard to relation between vegetation types and evapotranspiration, creating land cover map is an initial step by utilizing satellite images. This map has been made with the image classification method by ERDAS software. This geospatial software supplies tools for all remote sensing, photogrammetry, and GIS needs.

Image classification

With image classification we can convert remote sensing images into thematic data. Classification is based on the image pixels characteristics which have been done either by visual analysis or digital image classification. Visual analyses method related more to the interpreter's eye, despite the fact that digital image classification with help of computer instruction, try to interpret image's pixels in regard to certain conditions (Bakker et al., 2001). Digital image classification includes two different methods, unsupervised and supervised classification. In this research, a supervised classification method was selected using field observations for training samples. After creating the map with a 96% overall accuracy calculated by an independent control point set, the definition of each k_c factor for the land cover categories was the next step.

MODFLOW-NWT which will be explained in the next few pages requires PET. To convert reference evapotranspiration ET_0 to PET the single and dual crop coefficient are two main approaches to obtain k_c factor. In single crop coefficient k_c depends on growing stage and crop types as in equation 5, while in the dual approach the k_c factor is depends on evaporation and transpiration of the crop separately (Zehairy, 2014 & Weldemichiel, 2015). Having adequate data about vegetation and soil in the area enable us to use the dual crop coefficient method; nevertheless, for this study single crop coefficient approach has been applied.

$$\mathrm{PET} = k_c * \mathrm{ET_o} \qquad [5]$$

PET- potential evapotranspiration for each category [mmd^{-1}], K_c- crop coefficient [-]

Due to the definition of the reference evapotranspiration, with the k_c factor equals to 1 for grass. Six categories of land cover have been defined for this study area based on land use and vegetation including Building (residential area), Cereal, Maize, Trees, Grass, Heath and Water. The k_c value for each land use type has been defined based on the growing stage (Table4). This value for the residential area assumes to be zero.

(Allen et al., 1998) indicates the typical values of $K_{c\ ini}$, $K_{c\ min}$, $K_{c\ end}$ for each crop in the Table 4. Afterwards, temporal variability of the factors for each land cover type has been defined. The monthly values are summarized in Table 5 for the different vegetation covers. By obtaining the k_c factor and considering ET_0, PET was calculated for each month and then these values were averaged over the year. Finally, the calculated average PET values were used to create a raster map from the land cover map with 100*100 cell size.

Land cover	$K_{c\ ini}$	$K_{c\ mid}$	$K_{c\ end}$
Cereal	0.3	1.15	0.4
Trees	0.5-0.6	1-1.1	0.7
Grass	1	1	1
Maize	0.3	1.2	0.6
Heath	0.4	0.4	0.4
Water	1	1	1

Table 4: Single crop coefficients

Land cover	k_c factor											
	Jan	Feb	Mar	Apr	May	Jun	Jul	Aug	Sep	Oct	Nov	Dec
Cereal	0.3	0.3	0.3	1.15	1.15	1.15	1.15	1.15	0.4	0.3	0.3	0.3
Trees	0.5	0.5	0.7	1	1.1	1.1	1.1	1.1	1.1	0.8	0.6	0.5
Grass	1	1	1	1	1	1	1	1	1	1	1	1
Maize	0.3	0.3	0.3	0.4	1.2	1.2	1.2	1.2	0.6	0.6	0.6	0.3
Heath	0.4	0.4	0.4	0.4	0.4	0.4	0.4	0.4	0.4	0.4	0.4	0.4
Water	1	1	1	1	1	1	1	1	1	1	1	1

Table 5: Temporal variability of k_c factor

3.3.6. Evapotranspiration depth

According to Shah et al., (2007) applying variable rooting depth helps in subdividing vadose zone evapotranspiration and groundwater evapotranspiration since different vegetation type have different rooting depth. The model of Nyarugwe (2016) includes two category of rooting depths based on the dominant species in the catchment area: forest and heath. However, this assumption is based an oversimplification. For more improvement, the new model considers more land cover types. The existing

model set up has five major rooting depth categories based on the field work data collection and the confirmation of the Natural Resources department of ITC.

The rate of actual evapotranspiration varies linearly between zero and maximum rate of evapotranspiration in respect to the depth of the groundwater table: the maximum rate occurs when the groundwater table is at (or close to) the land surface and zero ET from the groundwater occurs at the extinction depth [EXTDP]. Figure 13 shows the schematic definition of implementing the extinction depth.

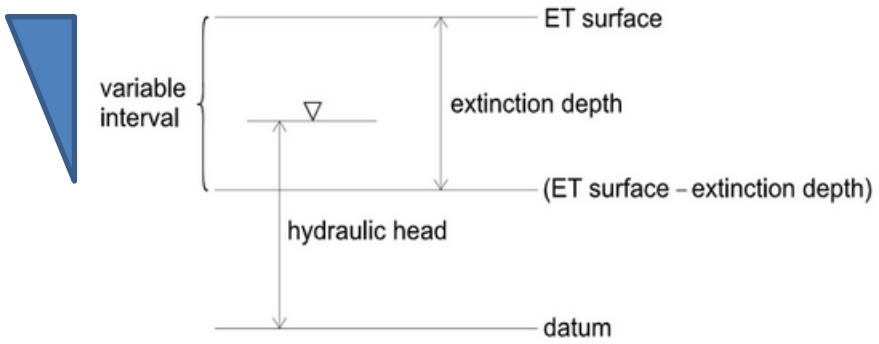

Figure 13: Schematic representation of ET estimation (Banta, 2000)

The spatial variation of EXTDP in this study was also estimated on the basis of the land cover map. The Aamsveen basin is mainly covered by grass, forest and heath lands. The EXTDP for grass lands which are about 28% of the whole research area was assigned 1.2 meter below ground surface. Trees which are representative of forest in land cover map covers 23% of total area and the EXTDP assigned for trees was 2.5m adopted from Shah et al.(2007). About 18.5% of the area is covered with the heath which is mostly in the heart of the Aamsveen wetland. The value assigned as an EXTDP for this land cover is 0.3m. For cereal and maize the EXTDP was adopted from literature. Mishra et al. (1997) suggested the EXTDP to be 1.45 for agricultural areas such as cereals and maize in this study. A raster map has been created in GIS environment including the different rooting depth based on the land cover.

3.3.7. Interception

Interception refers to precipitation which does not reach the ground because it retained by leaves and branches of plants. The rate of interception has direct relation with vegetation type and density. Interception has to be estimated in order to define the amount of precipitation that reaches the surface runoff and the amount of infiltrating water that reaches the groundwater system. In the previous steady state model of Nyarugwe (2016), the assumption is that there are two different land cover types (forest and heath) and the interception rate of those were based on (Fleming & Neary, 2004; Wang et al., 2007). In the here reported model, more land cover types are differentiated leading to a more detailed representation of the interception values.

The interception loss rate has been studied by different researchers. As an example, Leuning et al. (1994) consider 33% of rainfall as an estimation of interception rate on a wheat canopy. Fleming et al. (2004) estimated a range of 10-20% of rainfall for the same canopy. Moreover, Wang et al.(2007)accounted interception between 10 to 48% in diverse forests.

The rate of the intercepted precipitation was obtained using the land cover map of the study area (Figure 20). Table 6 demonstrates the values for each category in summary. In order to calculate total interception from different land cover types within one model grid, Equation [6] has been used:

$$I = RF * (I_1 * Area_1 + I_2 * Area_2 + \cdots + I_n * Area_n) \qquad [6]$$

$I =$ Canopy interception per grid cell [md^{-1}]
$RF =$ Rainfall [md^{-1}]
$I_n =$ Interception losses for land cover 'n' [%]
$Area_n =$ Area ratio covers by land cover 'n' [m^2]

Aamsveen Land cover	Interception [%]	Retrieved from literature
Cereal	14.4	(van Dijk & Bruijnzeel, 2001)
Tree	22.4	(Ghimire, Bruijnzeel, Lubczynski, & Bonell, 2012)
Grass	6.5	(Corbett & Crouse, 1997)
Heath	5	-
Maize	14.4	(van Dijk & Bruijnzeel, 2001)

Table 6: Interception loss rate applied to the different land cover types

3.3.8. Infiltration

Infiltration is the amount of water per surface area per time that percolates to the soil. The percolated water further becomes as recharge, or it can be routed as stream runoff. According to (Niswonger et al., 2006) infiltration further is divided into the different components such as runoff, evapotranspiration, unsaturated-zone storage, and groundwater recharge.

Generally speaking, the vertical hydraulic conductivity has a direct relation with infiltration rate which means greater vertical hydraulic conductivity caused the higher rate of percolation; however, this has a limitation. As far as the infiltration rate become higher than the hydraulic conductivity of soil, then the percolation gradually become less and the excess water comes along the surface and routed as runoff into streams. Using the Stream Flow Routing (SFR) package enable us to consider this fact. SFR package will be explained in the following section.

Recharge package accounts for the process of infiltration in this model. This package is a boundary package in which users are able to specify a maximum recharge rate over an area. In this package applying negative recharge value is also possible. A negative recharge, rate might be used to simulate a constant evapotranspiration rate. In the model, the settlement areas infiltration was assumed to be zero in order to indicate the impermeable surface. The rainfall over these regions is routed to the drains.

As far as we know, precipitation is one of the driving forces in both scenarios. Implementing two different precipitation values for two scenarios makes the infiltration rate vary for both. For applying the infiltration over study area, a raster map with the same cell size like the model (100*100) has been created. The average of daily rainfall from 2007 till 2011 and 2012 till 2016 has been calculated (Table 3). Although the rate of precipitation has slight fluctuation over time, in this model every piece of variation has an enormous effect to the model scenarios.

3.3.9. Hydraulic conductivity

In Nyarugwe's (2016) work the hydraulic conductivity zones were not considered equal in the pre-2011 and the post-2011. This neglects the fact that the soil properties of an area does not go to change in time. Considering two different K values for the same geology resulted in two separate models. Therefore, the whole model was reconsidered in this respect.

According to Campbell (1995), "Engineers frequently use soil texture to estimate saturated conductivity for design purposes." This statement is valid for modeling as well, so the results obtained from field work and laboratory were related to soil texture, since soil texture is available. In this sense, the soil grain sizes of each sampeling point of the field work were defined from the https://www.soilgrids.org database and the saturated corresponding hydraulic conductivity was calculated based on the Campbell equation (Equation 7). This equation can never correctly predict the saturated conductivity of a soil which has interconnected cracks and holes.

$$k_s = C \exp(-6.9\, m_c - 3.7 m_s) \qquad [7]$$

Where-C is constant equal to 4×10^{-3} [kg.s.m^3]; m_c is clay mass fraction; m_s is the silt mass fraction

After calculating the k_s value for each point, the values of field work measurements and the theoretical calculation were compared. The results were quite acceptable with one order of magnitude differences. In this regard, a soil map based on this equation for whole study area was created in GIS environment. The reclassification of the k_s value for making the conductivity zones were done based on the general knowledge of soil properties over the area. Finally, the area divided into 5 different zones, including the peat layer. In the following the flowchart summarized the process (Figure14). More explanation is available in the result and analysis chapter.

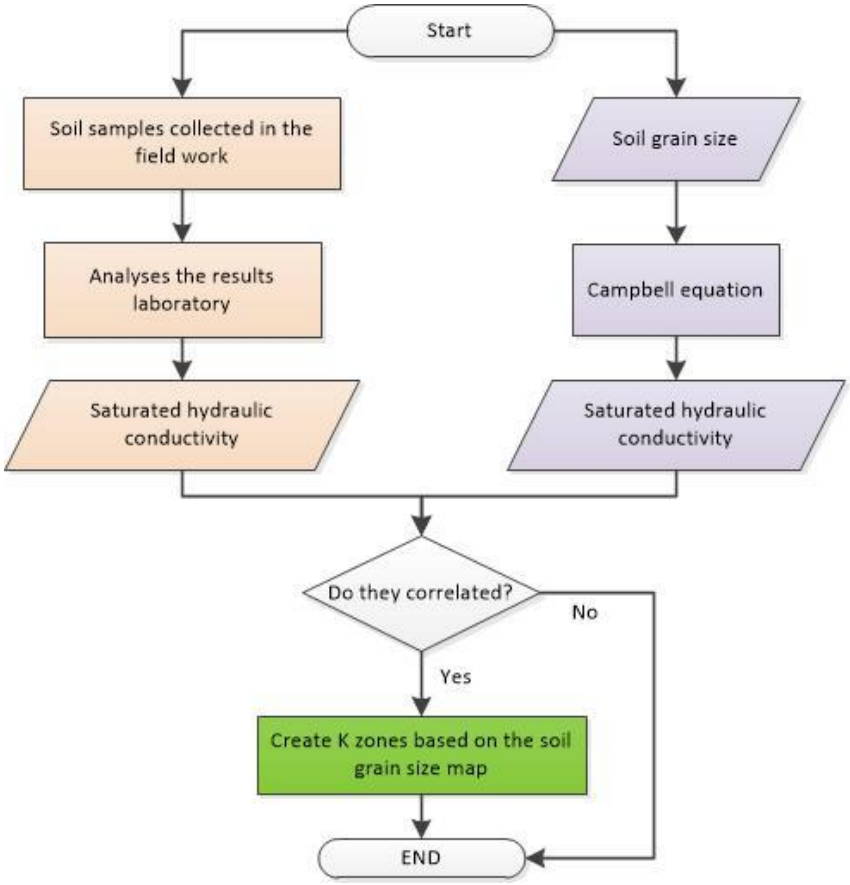

Figure 14: Flowchart related to saturated hydraulic conductivity value and zones

3.3.10. Stream discharge

The main creek in this area is the Glanerbeek. Discharge data from this stream in the previous study was used as channel flow input and output from the wetland system (Nyarugwe, 2016). The model requirs stream width, streambed elevation and thickness, channel roughness, stream slope, and runoff volume.

The Vechtstromen provided the gauging data of the wire for the period of 2012-2016.The data set contains hourly measurements, but unfortunately with the data gap in March-June 2015(Figure 15). This data set is suitable to compare the simulated discharge value the new scenario. There is no available information regarding the old scenario (2007 till 2011), since this measurement station was established in 2011. Thus, the discharges value in this study were used only to validate the model calibration.

There is also no measurement available in the downstream part of the Glanerbeek for both scenarios. Figure 15 presents the estimated discharge value of Glanerbeek Melodeistraat which is located nearby the border. These estimated values do not consider the drain discharges since it is located before the stream and drain junction (Figure 16). Therefore, there is no real measurement for the outlet of the water flow in this study area.

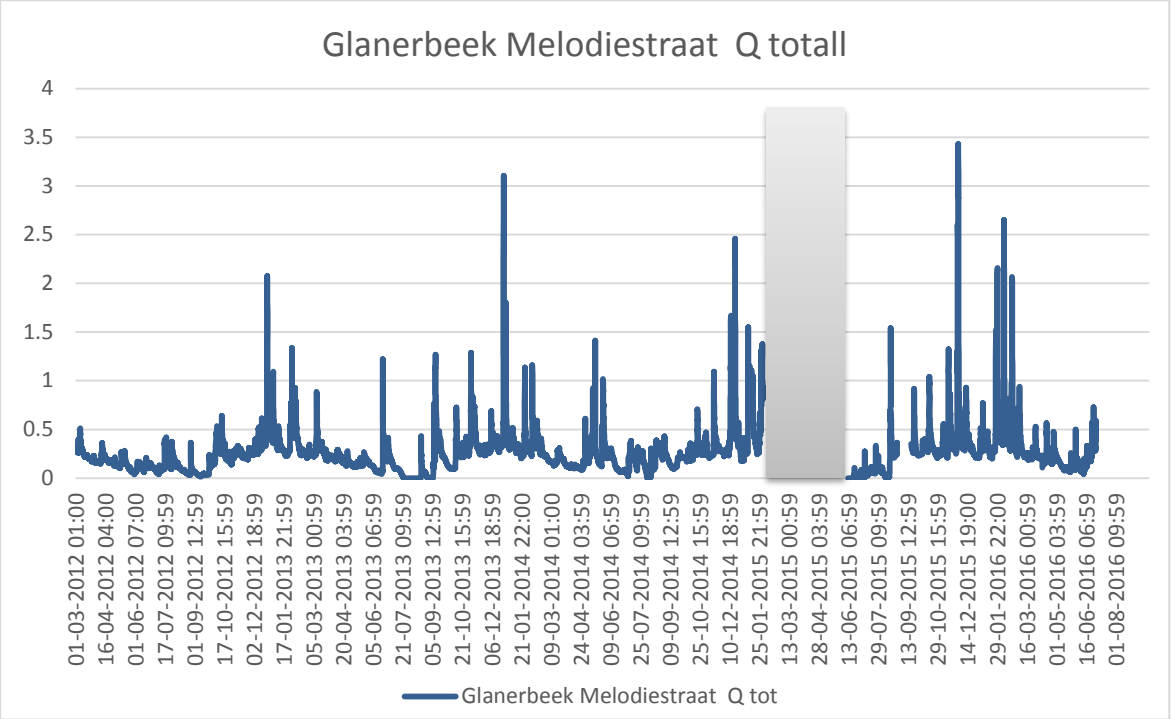

Figure 15: Estimation of downstream discharge values for the post-2011 scenario

3.4. Conceptual model

Development of the conceptual is based on understanding the field problem and means that translation of the problem into a simple form in order to analyze it. Most groundwater problems are addressed with a mathematical model developed from the conceptual model (Anderson, Woessner, & Hunt, 2015). Formulating the conceptual model unavoidably needs simplifications, which lead to discrepancies between the system and its simplified representation. In this sense, special attention needs to be paid to the implementation of the most important aspects over the study area. In this study, in order to reduce the error and represent the real situation, some modifications were implemented in comparisson to former model by consulting the water board (Vechtstromen). As mentioned before, two scenarios were modeled. In the pre-2011 scenario, a central drain is the main water course, which drained the water from the wetland through the tube. In 2011, the central drain has been blocked and the water was diverted through a gauging weir into the river bed of the Glanerbeek, on the north-western edge of the wetland. Nevertheless, the conceptual model is based on the one developed by Nyarugwe (2016), but some small modification were implemented. This model includes four main parameters: hydrostratigraphic units, flow system pattern, water balance, and boundary conditions.

- **Hydrostratigraphic units:**

  The geological features which have similar hydrogeological properties are summarized in a hydrostratigraphic unit. This means, that stratigraphic units can be combined into one unique hydrostratigraphic unit or act as an independent unit based on the hydrological formation of the layer.

The structural hydrostratigraphic layers and thickness were adopted from Nyarugwe (2016). The study area has two modeled hydrostratigraphic units besides the underlying boulder clay unit which has a very low hydraulic conductivity. This layer is considered as an impermeable lower boundary for the model. This consideration is due to the Anderson et al. (2015) statement that no-flow boundary assign to the hydrological unit when the transmissivity of that unit has more than two order of magnitude differences. Furthermore, the upper layer is a peat layer with maximum 1-meter thickness and the lower layer is a sand layer with nearly 10-meter depth.

Figure16 shows the hydrostratigraphic unit in the Aamsveen wetland by the cross-section CC'(Figure 1c & 5). Based on the above definition, the upper layer considered as an convertible aquifer like the lower layer. In modeling set up convertible means where cells can convert from confined to unconfined conditions.

❖ **Flow system pattern and water balance**

The aquifer of this study area is shallow which is recharged by precipitation. The outflows are groundwater evapotranspiration and lateral groundwater flow on the north and north-eastern boundary (Bell, J.S. & van 't Hullenaar, 2015). Water tends to flow in regard to altitude differences. The direction of flow is started from south, near the border with Germany to the north part of the study area. In other words, groundwater flows from the upper big pits through the sand layer in the northwest down to the Glanerbeek.

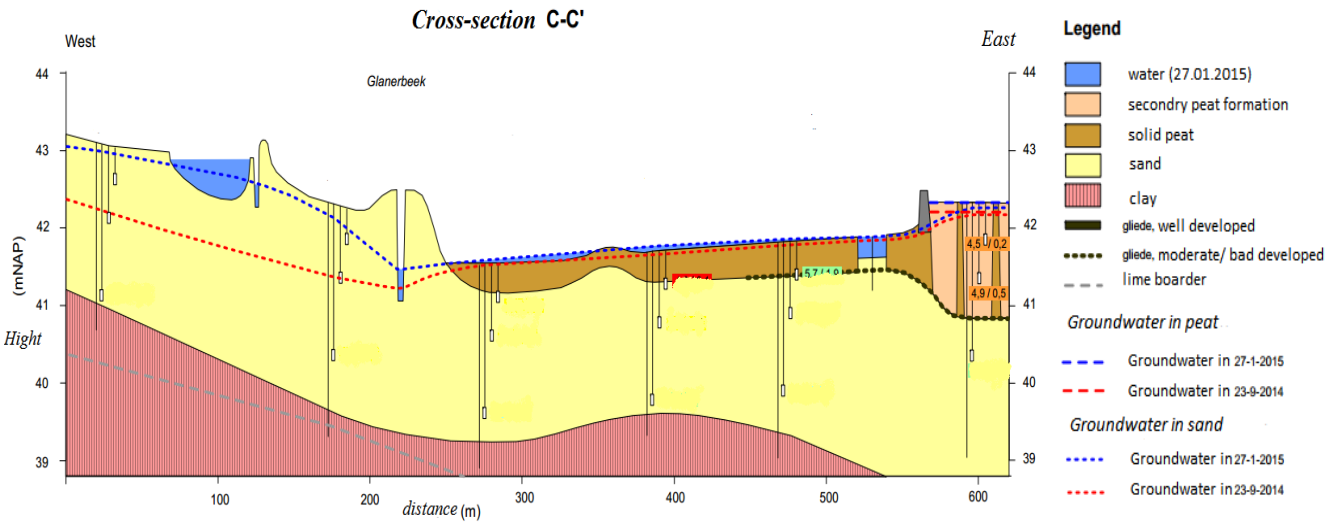

Figure 16: Cross section C-C' of the Aamsveen wetland in relate to Figure 6b. Source (Bell, J.S. & van 't Hullenaar, 2015)

❖ **Boundary conditions**

Assigning the boundary for the groundwater modeling would be an important task. Boundary conditions are known as either external boundary or internal boundary. In this study area, external boundaries define as no-flow boundary in whole direction except in the north part which is drain boundary. In the previous study by Nyarugwe (2016), boundaries around the study area have been considered as a no-flow boundary; however, by consulting to the Overijssel Water Border in the Netherlands, in the North part of the study area there is a drain ditch along with the railway. With the help of this ditch at the time groundwater level become higher, the water route out of the area. For all the layers of the model, the same external boundary has been used. Figure 17 shows the study area location with the external and internal boundaries for the post-2011 scenario and

for pre-2011 scenario. The internal boundaries like some part of drain and stream and new reservoir were changed in the post-2011 scenario after the modifications.

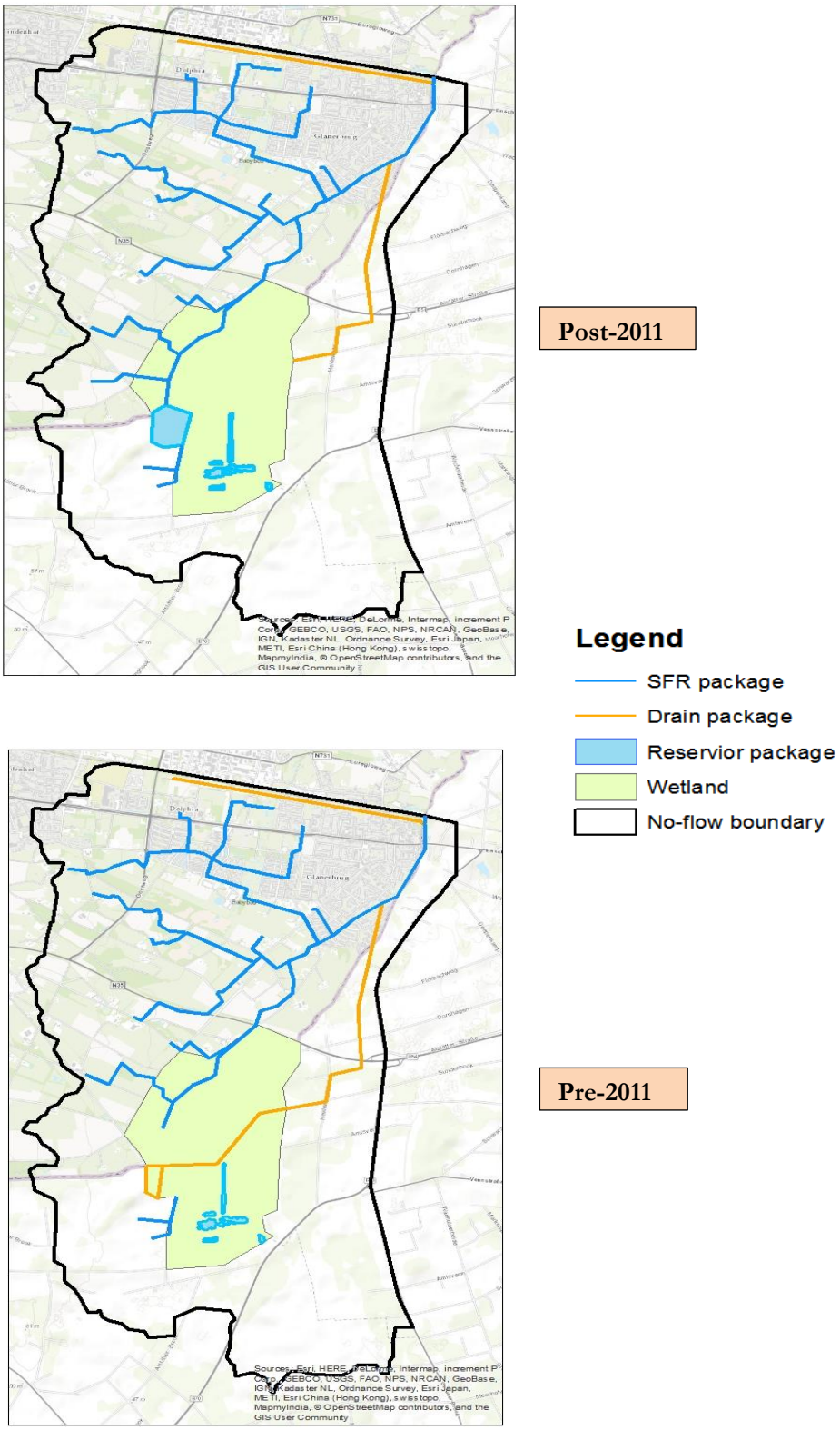

Figure 17: Defining external and internal boundaries of the study area in pre-2011 and post-2011

3.5. Numerical model

According to (M. P. Anderson et al., 2015), the next step after developing the conceptual model is building a numerical model of the system. The numerical groundwater models have been developed to solve the equations of groundwater flow. In numerical modeling, software selection, design of the grids, layer definition and boundary conditions are included.

3.5.1. Software selection

One of the most common codes for solving the groundwater flow problems is MODFLOW. A code is a set of equations and methods to solve a problem which is usually programmed into a machine code (M. P. Anderson et al., 2015). The MODFLOW-2005 is a 3D finite difference model which can be used for modeling the steady-state and transient flow in any types of aquifer layers (e.g. confined, unconfined or a combination of confined/unconfined). The fundamental function of MODFLOW is Equation 8 which includes three dimensional incompressible groundwater flows through a porous medium.

$$\frac{\partial}{\partial x}(K_x \,.\, \frac{\partial h}{\partial x}) + \frac{\partial}{\partial y}\left(K_y \,.\, \frac{\partial h}{\partial y}\right) + \frac{\partial}{\partial z}\left(K_y \,.\, \frac{\partial h}{\partial z}\right) + W = S_s . \frac{\partial}{\partial t} \qquad [8]$$

Where K_x, K_y and K_z are hydraulic conductivity values [LT^{-1}] in x, y and z directions, respectively. Moreover, h is the potentiometric head [L] and W is the volumetric flux per unit volume [T^{-1}] which represents sink and/or sources. Negative values of W show that water leaves the system and positive values of W show that water flows into the system. S_s is the specific storage [L^{-1}] which in steady state modeling it is ignored; and t is representing time [T].

MODFLOW-NWT is a Newton formulation of MODFLOW-2005 which can solve the most complex equations by considering the nonlinearities in an unconfined aquifer (Niswonger, Panday, & Ibaraki, 2011). Selection of the software depends on the environment in which the groundwater system is being modeled. A graphical user interface (GUI) is an intermediate between the user and the computer code.
In this research, the groundwater system was modeled using MODFLOW-NWT under the GUI ModelMuse 3.8.1.

3.5.2. Grid design

Designation of the grids cell size in a groundwater model is one of the important steps to represent the spatial extent of the model sufficiently and to have a reliable simulation. On the one hand, large grid cell size can increase the computation speed and decrease the simulation time, whilst on the other hand, it leads to having a very general model in which a lot of details are ignored. Moreover, small grid cell size can improve the accuracy of the model by considering more details which are in reality, although, the required time for simulation increases. Therefore, considering both aspects (simulation time and accuracy) is needed to design the grid cell sizes. In this study, the grids are block-centred with a size of 100m*100m and there are 76 rows, 46 columns and totally 3496 cells in each layer. The model set up is based on the Universal Transverse Mercator coordinate system (UTM).

3.5.3. Head Observation Package

The application of this package makes comparing the observed heads possible. The simulated heads in the location of observation points are calculated by interpolating the values from the nearest cells.

3.5.4. Recharge Package

The Recharge Package can simulate a spatially distributed specified flux and the rates are multiplied by the horizontal area of each cell to calculate the volumetric flux rates. This package allows the user to input an array of flux values which covers the entire of the study area. It is also possible to specify the layer to which recharge is applied.

3.5.5. SFR2 Package

SFR2 Package is designed to study the interaction between streams and the groundwater in addition to the flow and storage in the unsaturated zone below the stream. The functionality of River Package and SFR2 Package is somewhat similar. In River Package flow can occur from the stream to the groundwater or vice versa depending on the difference in river stage and water table although, in SFR2 Package water flows through the streams(Niswonger & Prudic, 2005). One of the advantageous of using SFR2 Package is considering the flow diversion and simulating the stream connections. By applying ordinary numbers to each segment, the connection between streams is being adjusted (Zehairy, 2014).

Generally, the amount of water flows between two sources is being calculated by using Darcy's equation and assuming uniform flow between them. SFR2 Package can calculate the stream depth of each segment by different methods: a) user can define the value of stream depth directly, b) by using the Manning's equation for rectangular channels, c) by using relationships between depth-discharge and width-discharge and d) defining the values of stream depth and width of the channel at some observation points and interpolating the values in between automatically. Moreover, the user can add (or subtract) water to (or from) streams based on the precipitation, runoff and evapotranspiration data for each segment and assign to the model (Prudic, Konikow, & Banta, 2004).

The simulation of unsaturated flow beneath the streams is being computed based on kinematic wave approximation to Richard's equation. In this method, horizontal flow component is disregarded and it is assumed that all amount of water flows in the vertically downward direction (Teketel, 2017) and therefore, direction of filling the unsaturated pores is downward. Seepage from the stream could be either horizontal or vertical. It is also assumed that the diffusion is neglected and the zones are homogeneous and isotopic.
In SFR2 Package, input data includes stream flow network, streambed top, streambed thickness, streambed hydraulic conductivity, stream width, bank roughness, channel roughness, stream slope, saturated and initial water contents, maximum vertical hydraulic conductivity in the unsaturated zone and flow into the upstream end. The volumetric water discharge is being calculated based on Equation 9:

$$\mathrm{Q}_l = \frac{KWL}{M}(h_s - h_o) = c(h_s - h_o) \quad [9]$$

Where Q_l is volumetric flow [m^3d^{-1}] between a stream section and aquifer volume; K is the hydraulic conductivity [md^{-1}] of streambed sediments; W is width [m] of the stream; L is length [m] of the stream; M is thickness [m] of the stream deposits; h_s is the stream head [m] and h_l is the aquifer head [m]; and C is riverbed conductance [m^2d^{-1}].
Regarding Equation 9, the interaction between the stream and aquifer depends on the head difference and conductance. If the groundwater table is higher than the stream stage (Figure 18a), water flows to the stream and if the groundwater table is lower than stream stage (Figure 18b), water flows to the aquifer. Although, when the water table is lower than streambed (Figure18c), flow is independent of the aquifer head. For these conditions, Niswonger and Prudic (2005) suggested estimating the stream leakage flow by calculating head gradient between stream head and streambed. The authors assumed that the hydraulic

head at the bottom of the stream is equal to the streambed elevation. Moreover, the rate of streambed leakage does not exceed the saturated hydraulic conductivity value.

In this research, the ordering map for the streams was generated and imported to the model for defining the river reach connectivities. In order to simplify the model, all the streams and drains were considered having rectangular sections and the streambed thickness was assumed 0.2 m. The hydraulic conductivity for each zone is different and the values were adjusted by doing the model calibration. Moreover, Manning coefficient for the streams assumed to be 0.035.

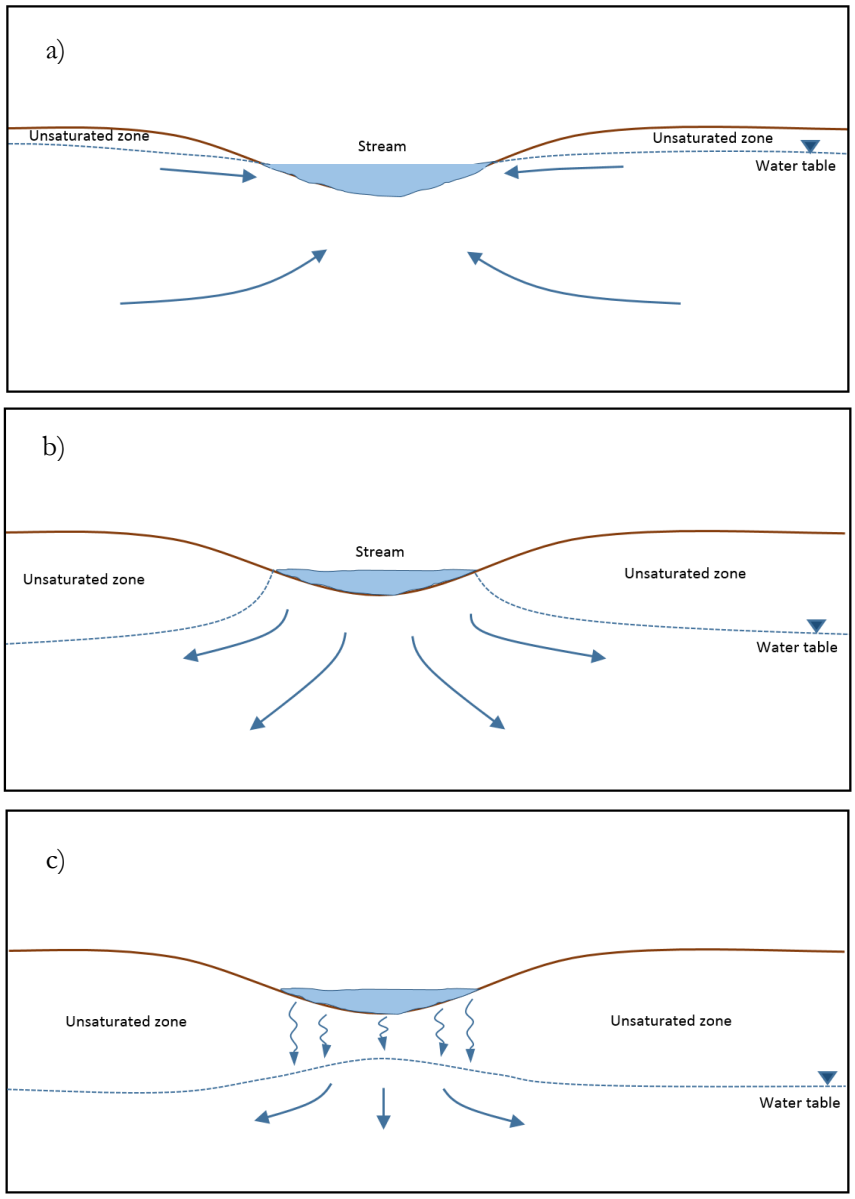

Figure 18: Stream and aquifer interaction a) Gaining stream [water from groundwater] b) losing stream [water flows to the groundwater] c) Dry stream (leakage)

3.5.6. Error assessment

In order to find the good match between simulated and observed heads, model calibration is essential. In this study, hydraulic conductivity was adjusted by trial and error method until observed and simulated heads had a good match. Although, it should be considered that it is laborious to find the exact values due to some uncertainties which are associated with the groundwater models. The main sources of these uncertainties are observed data, model parameters, conceptual model and boundary condition (Wu & Zeng, 2013).

Moreover, understanding the effect of these uncertainties on behaviour of the model was done based on a sensitivity analysis and the parameter to which the model is the most sensitive were defined.

To assess the reliability of the calibration residuals, three error metrics were adopted. Root Mean Square Error (RMSE), the Mean Error (ME) and Mean Absolute Error (MAE) which are given in Equation 10, 11 and 12, respectively.

$$\mathrm{RMSE} = \sqrt{\frac{1}{n}\sum(H_{OBS} - H_{sim})^2} \quad [10]$$

$$\mathrm{ME} = \frac{1}{n}\sum(H_{OBS} - H_{sim}) \quad [11]$$

$$\mathrm{MAE} = \frac{1}{n}\sum|H_{OBS} - H_{sim}| \quad [12]$$

Steady-state models need only a single set of calibration data and produce only one set of result.

3.5.7. Sensitivity analysis

Estimation of aquifer parameters from field measurements of hydraulic head is always one of the most challenging tasks in groundwater modeling. With this intention, analyzing the uncertainty in modeling based on spatial and temporal variation, number and type of model parameters and boundary conditions become a crucial dispute. Utilizing sensitivity analysis in this research enables us to evaluate the model response on changes/inaccuracies in certain parameters. Generally speaking, sensitivity analysis in trial and error model calibration involves incremental changes in one parameter while holding the other parameters constant (McElwee, 1987).

4. RESULT AND ANALYSES

4.1. Potential evapotranspiration

As mentioned in the methodology, there is only one meteorological station with the daily evapotranspiration value for the total study area. The monthly averages of ET_0 for two scenarios are shown in figure 19. The overall average of ET_0 for the pre-2011 period was 1.57 mmd^{-1}, and for post-2011 this value was 1.61 mmd^{-1} estimated. The difference between these two average values is subtle; so that, to make the difference more tangible, creating a land cover map plays an important role. Apply a different driving forces in scenarios could evaluate the model better.

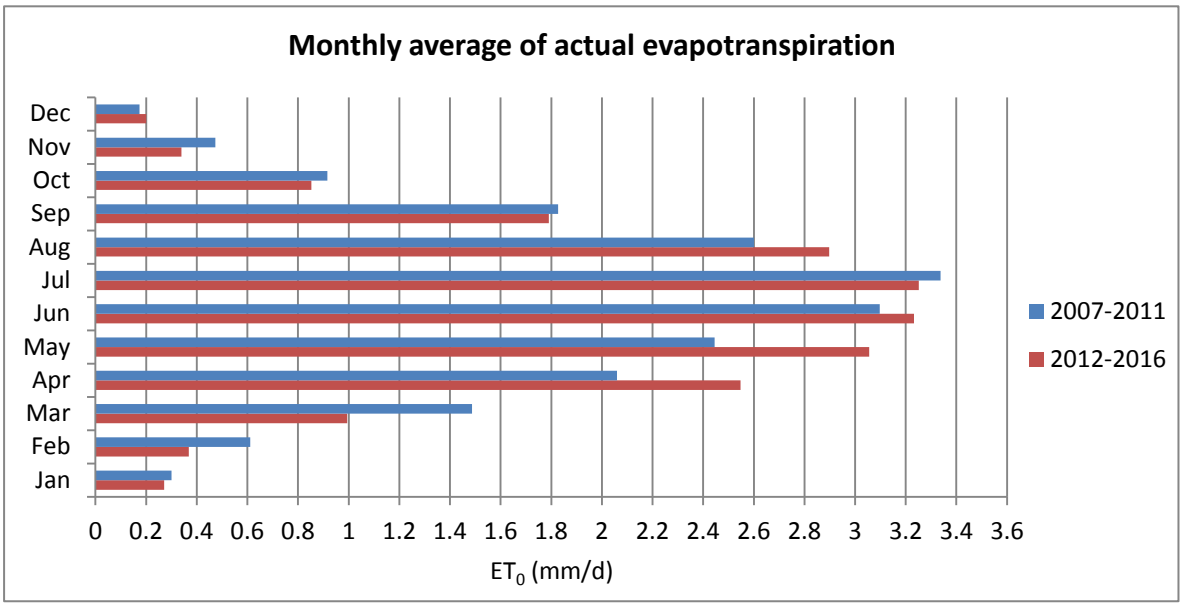

Figure 19: Monthly average distribution of ET0 [md^{-1}]

The approach of assigning PET to the land cover classes is described in 3.3.4. In order to create land cover map, the image classification with the image obtained from Sentinel-2A satellite 2015 was done. The land cover map was produced (Figure 20) including seven classes: building, water, cereal, maize, heath, grass, and trees. In Figure 21, the percentage of coverage in the study area is shown. Grass as a landcover contributed the major part of this research more than 28%. Most of the Aamsveen wetland is covered with trees and heath; however, the northern part of the study area is residential.

Land cover map

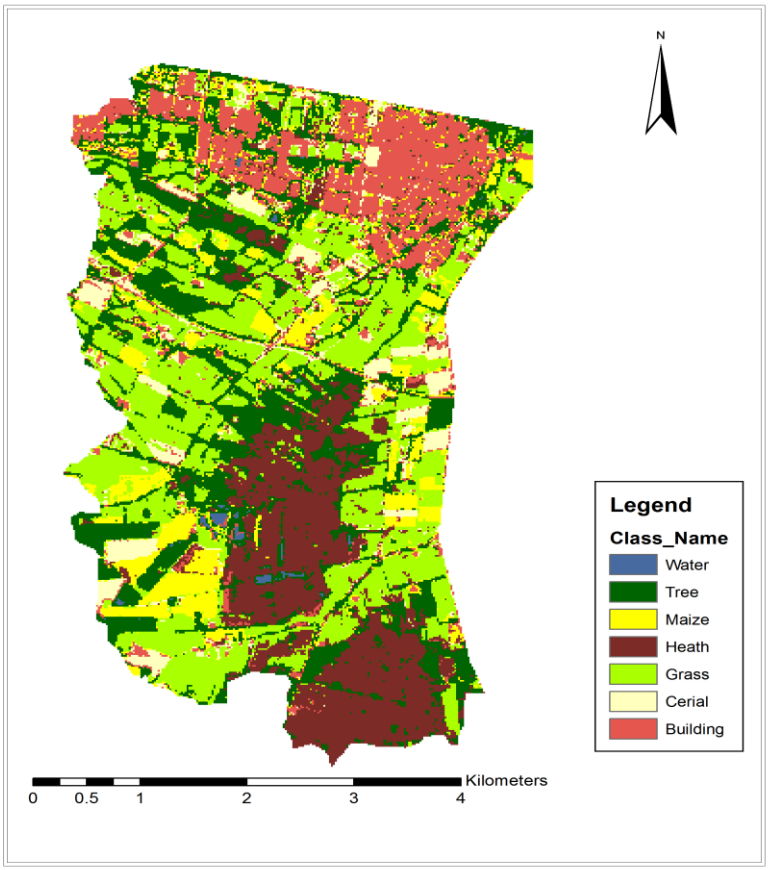

Figure 20: Land cover map of the study area obtained from image classification

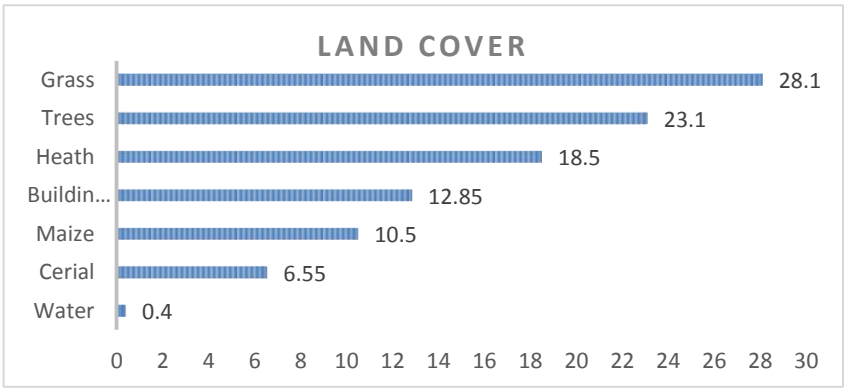

Figure 21: Percentage of area coverage of Aamsveen basin

The accuracy assessment based on the field work knowledge and helping points from NRM Department of ITC showed a good match with the real situation: an overall accuracy of 96%. Figure 22 is the accuracy table of the land cover classifications used in this study area.

CLASSIFICATION ACCURACY ASSESSMENT REPORT

Image File : d:/data/landcover/classification_sayeh/classified1.img
User Name : Lenovo
Date : Wed Jan 25 17:29:51 2017

ACCURACY TOTALS

Class Name	Reference Totals	Classified Totals	Number Correct	Producers Accuracy	Users Accuracy
Unclassified	0	0	0	---	---
Cerial6	15	19	15	100.00%	78.95%
Building20	49	48	48	97.96%	100.00%
Tree11	45	48	45	100.00%	93.75%
Grass15	63	57	57	90.48%	100.00%
Heath6	9	9	9	100.00%	100.00%
Maize9	20	20	20	100.00%	100.00%
Water8	7	7	7	100.00%	100.00%
Totals	208	208	201		

Overall Classification Accuracy = 96.63%

----- End of Accuracy Totals -----

Figure 22: Accuracy assessment report

In this study, the reference evapotranspiration (ET_0) derived from the KNMI Weather Station. To calculate PET for the different land cover and vegetation classes, the temporal distribution of K_c factor based on the vegetation growing stage was obtained from the FAO-56 method. Table 7 indicates the average of the results from the K_c factor (Table5) multiplied by ET_0 for each landcover type, for the two scenarios. For water, based on the reference evapotranspiration definition, the PET was considered the same as of the grass. In this study, residential area assumed to have zero evapotranspiration.

Evapotranspiration (monthly average)[mmd^{-1}]	Cereal	Building	Tree	Grass	Maize	Heath	Water
Pre-2011	1.57	0	1.68	1.61	1.52	0.65	1.61
Post-2011	1.46	0	1.61	1.61	1.4	1.78	1.61

Table 7: Monthly average evapotranspiration for each land use in Aamsveen basin [mmd^{-1}]

4.2. Hydraulic conductivity value and zones

As mentioned in section 3.3.9, the hydraulic conductivity data from the fieldwork was compared to the calculated saturated conductivity using equation 7, based on the texture data of the Dutch national source data base. The measured values of saturated conductivity in the fieldwork and the calculated saturated conductivity by testing and applying Campbell equation is given in Table 8. The comparison shows systematically higher values of the field samples by factor of 2-11 than of the calculated ones. This evaluation only carried out for the samples that were collected from the Sandy area (six out of nine) since the soil grid website does not include the peat zone in its classification.

Sample No.	Soil structure			K(md^{-1}) Measured	K(md^{-1}) Calculated	Depth (cm)
	Sand (%)	Silt (%)	Clay (%)			
1	65	25	10	7.61	0.6873	40-45
2	63	26	11	6.82	0.6182	60-65
3	61	27	12	2.68	0.55	65-70
4	69	22	9	2.8	0.82	70-75
5	67	22	11	1.27	0.7	52-57
6	61	27	12	1.08	0.55	70-75

Table 8: Field work point values of saturated hydraulic conductivity in comparison with the calculated saturated conductivity

The difference between the results could be due to either the uncertainty of the field work measurements or the uncertainty of the soil texture fraction database. The soil texture data base includes the texture of the whole top 2 meters in one category whilst the field data were collected from a shallower zone. Due to the low number of compared values, there is no clear relation shown between the two data sets. The average difference is about a half order of magnitude, which is well within the theoretical conductivity range of sand deposits. It can be concluded that in spite of the differences, the texture data of the Dutch national soil data base in an acceptable starting point for the mapping of the saturated hydraulic conductivity of the sand layer, keeping in mind, that during the model calibration, these values should be increased, where needed.

The raster files of silt, sand, and clay distribution over the study area were downloaded from the Dutch national soil database. A hydraulic conductivity map was generated in ArcMap using the Campbell equation. Evaluating the results of soil texture calculation with the field work data confirm the approach. Based on this map, four saturated conductivity zones were assigned to the model for the sand zones. For areas without peat coverage, values are apparently the same for the first and the second layers. Where peat exists in the first layer based on the pervious study and the experiment during the field work (figure 23) the hydraulic conductivity of the top layer corresponds to the peat. The final zones of k_h created with the theoretical formula are in line with the overall soil map of the study area.

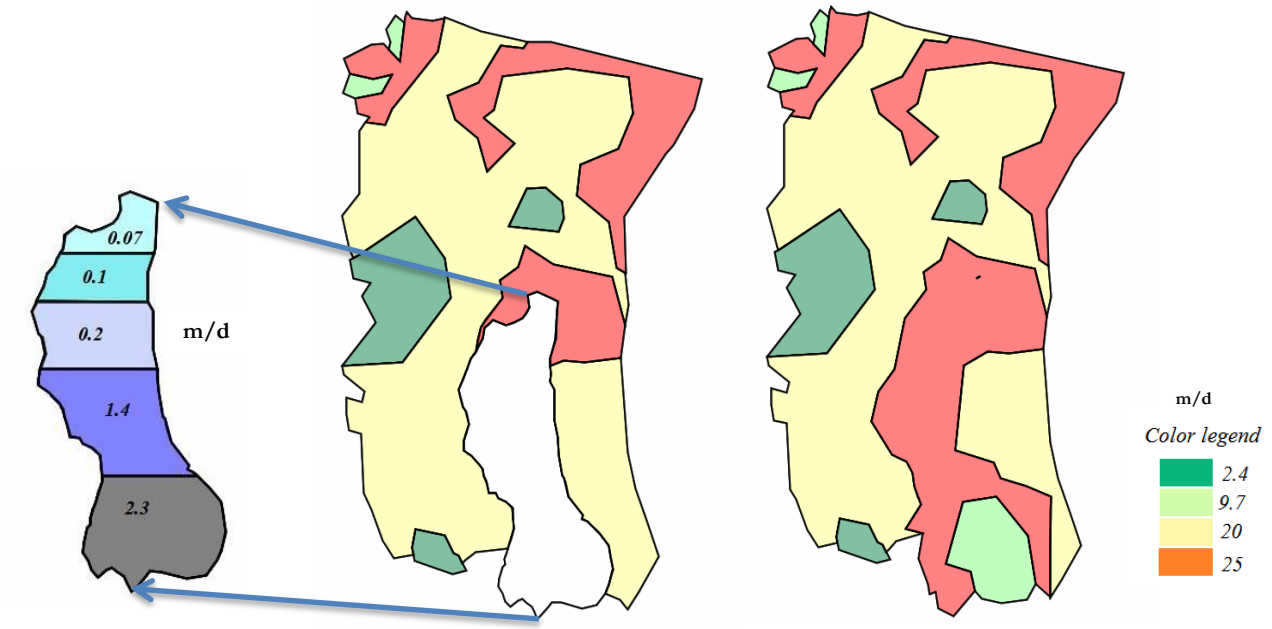

a) Zones for peat b) Zones for **first** layer c) Zones for **Second** layer

Figure 23: Horizontal hydraulic conductivity (K_h) distribution map of the study area after the calibration [md^{-1}] for the first and second layer in detail

According to the field work measurements and analyses in the laboratory, the vertical hydraulic conductivity (K_v) would be $^1/_3$ of the horizontal hydraulic conductivity (K_h). In the first hydrostratigraphic layer which is a peat layer with the depth of 0.7 to 1.1 meter, the horizontal and vertical values were assumed to have the same value.
The zones and spatial distribution of K_h were shown in figure 23. The results of steady state calibration demonstrate that K_h varies from 2.4 to 25 md^{-1} in the sandy region and 0.07 to 2.3 md^{-1} in the peat region of Aamsveen basin. The hydraulic conductivity zones in peat layer were assigned manually. The K_h values trend in the peat zone shows the increasing hydraulic conductivity to the south of study area.

In figure 24 the values of hydraulic conductivity according to the soil texture from FAO shows that the majority part of the study area covered with medium sand textured. This is in line with the geology of the area. Some small part of the western side would be also defined by fine sand.

To put in a nutshell, the value and zonation of this study in compare with former study which had an arbitrary zonation of K value, has one big step forwards. As figure 25 shows, in former modeling attempt the k zones consider to be different by shape and value; while this is in contradict to the geology of one unique are. The hydraulic heads value became more realistic in current model. Apart from that, the first layer of his model only consider the peat area which means the cells which are over the second layer (sand) were inactive.

K and μ values according to the soil texture and structure

Texture (USDA)[1]	Structure	μ	K (m/d)
C, heavy CL	Massive, very fine or fine columnar	0.01–0.02	0.01–0.05
	With permanent wide cracks	0.10–0.20	> 10
C, CL, SC, sCL	Very fine or fine prismatic, angular blocky or platy	0.01–0.03	0.01–0.1
C, SC, sC, CL, sCL, SL, S, sCL	Fine and medium prismatic, angular blocky and platy	0.03–0.08	0.1–0.4
Light CL, S, SL, very fine sL, L	Medium prismatic and subangular blocky	0.06–0.12	0.3–1.0
Fine sandy loam, sandy loam	Coarse subangular block and granular, fine crumb	0.12–0.18	1.0–3.0
Loamy sand	Medium crumb	0.15–0.22	1.6–6.0
Fine sand	Single grain	0.15–0.22	1.6–6.0
Medium sand	Single grain	0.22–0.26	> 6
Coarse sand and gravel	Single grain	0.26–0.35	> 6

[1] C: clay; L: loam; S: silt; s: sand.
Source: Adapted from FAO, 1980,

Figure 24: Hydraulic conductivity value according to the soil texture and structure by FAO (Van der Molen et al.(2007)

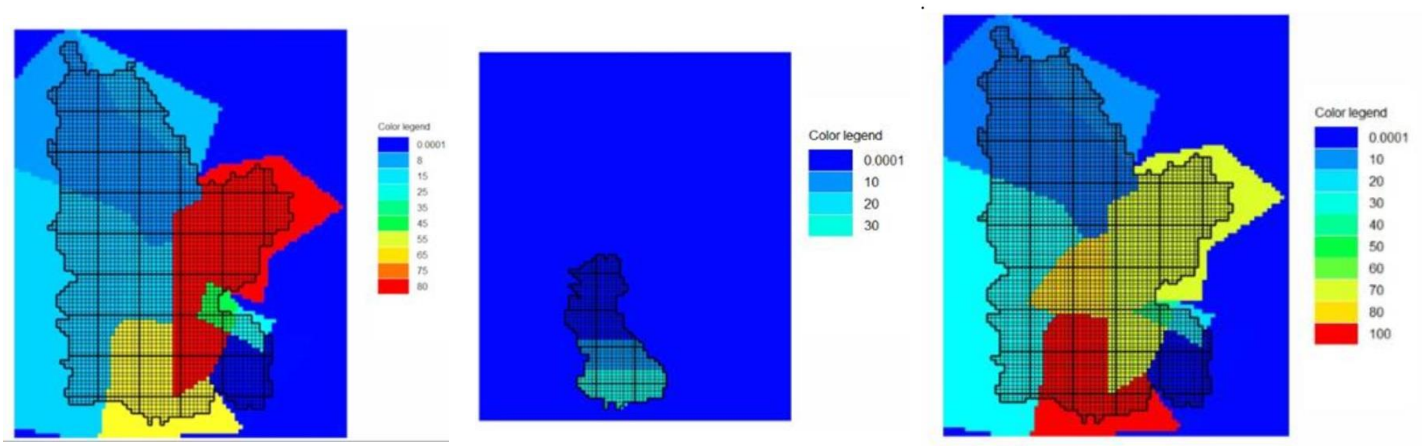

a) b) c)

Figure 25:Hydraulic conductivity zones of Nyarugwe work a) Hydraulic conductivity zone of the post-2011 model b) hydraulic conductivity of the first layer c) hydraulic conductivity zones of pre-2011 model

4.3. Steady–state model calibration

Model parameters estimated for the steady-state calibration was hydraulic conductivity and drain conductance. It is important to keep in mind that the drain is existed in pre-2011 scenario. The calibration target was to simulate the groundwater hydraulic head through the trial and error method. Within the calibration, simulated discharge values also compared to the available calculated discharge value. The results show that the values are quite close. The calibrated steady-state model for the inputs of the post-2011 period should also work for the pre-2011 period. The initial steps for calibration were taken into account as the following explanations. This part divided into three main subsections which are head calibration, residual, and the water balance of the whole study area. Each part includes more discussion regarding each scenario and compares the current model results with former models created by Nyarugwe (2016).

4.3.1. Head calibration

The head calibration for the model started from the post-2011 scenario's inputs. As soon as the calibration reached a satisfactory level, the model was tested with the pre-2011 scenario. After the first calibration attempt, the results showed a good trend; however, the model still needed some fine tunings. These steps were repeated until the model showed good results for both periods.

Figure 26 and 27 show the scatter plots of the measured versus the simulated heads of the two scenarios for 9 points with a trend line. The results show the regression coefficients for both scenarios, which are 0.989 for post-2011 and 0.979 for pre-2011. The results are in line with the recommendation of Hill (1998) that the R^2 should be more than 0.9. The observation points are in both modeled layer.

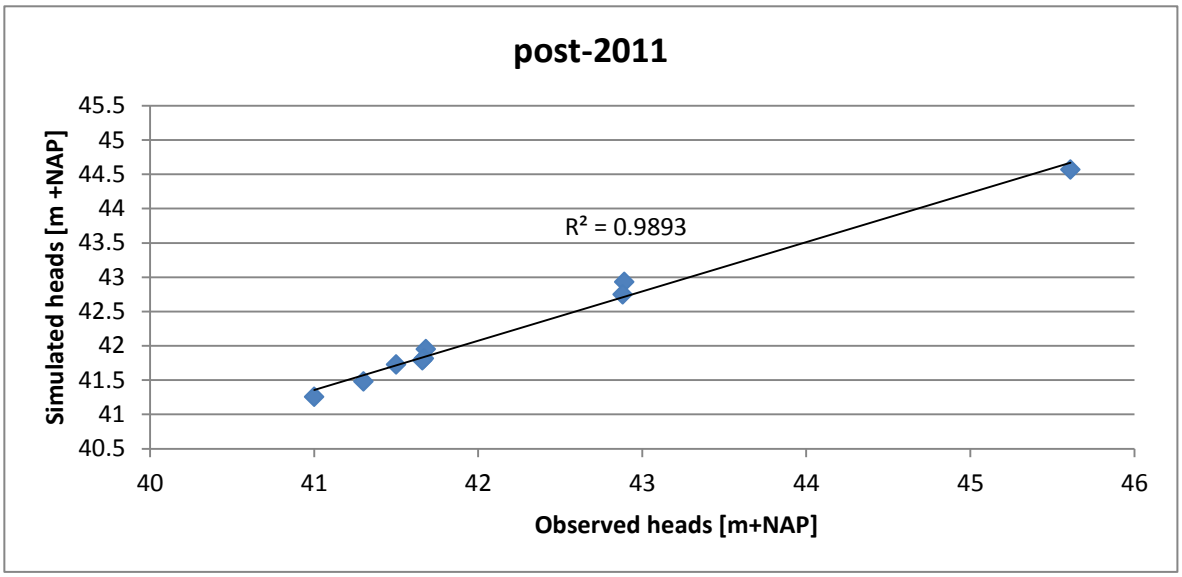

Figure 26: Relation between simulated heads and observed heads in the study are for the2011-2016period

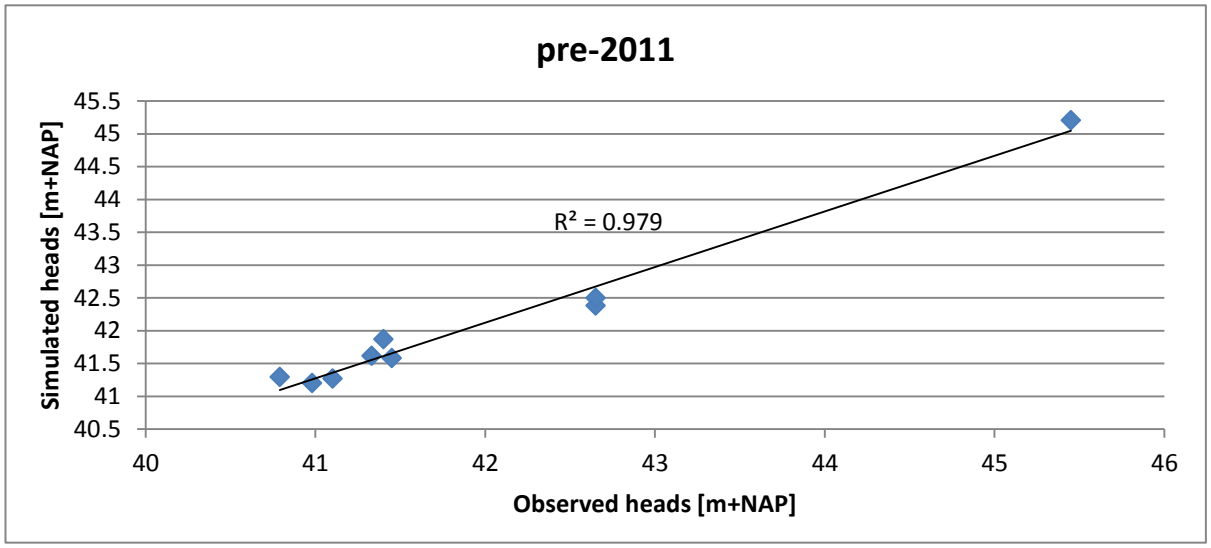

Figure 27: Relation between simulated heads and observed heads in the study are for the2007-2011period

After the ultimate model calibration the mean error (ME), mean absolute error (MAE) and the root mean square (RMSE) were calculated between the simulated and average observed heads. The observation heads for each period has a different value so that two series of error assessments were done. For the post-2011 scenario, the RMAE, MAE, and ME are 0.389, 0.267, and -0.005 m, respectively and the total head difference of the observations during the present period is 4.61m. For pre-2011 also the RMSE, MEA, and ME are 0.292, 0.271, and -0.124 m. In the drain scenario (pre-2011) total head difference of the observations is 4.66 m. According to Anderson et al. (2015), in order to do the error assessment, the ratio of RMSE to total head differences should be less than the 10% of the total head changes. This calibration coincides with this criterion for both scenarios, which means the model has reached the target and could simulate other water management modifications.

In Tables 9 and 10, the details of the observed heads, simulated head values, and the residuals of 9 observation wells are shown. All the error parameter values, as mentioned in the previous paragraph are satisfactory. In this model, most of the simulated heads are more than the observed heads this means there is a bit excess water in the model and better calibration could create a better simulation. It is necessary to mention that the model has a reasonable simulation for all piezometers. The only high discrepancy is in the piezometer B35A0194 with almost one meter less head simulation in the post-2011 scenario. However, in pre-2011 these piezometers have the same discrepancy as other piezometers. The Nyarugwe (2016) model had similar results. Revealing the reasons of this discrepancy would need field investigations, therefore, this was beyond the possibilities of the present work.

Post-2011 scenario					
Bore hole ID	Observed head[m]	Simulated head[m]	$(obs - sim)$	$\|obs - sim\|$	$(obs - sim)^2$
B35A0184	42.890	42.926	-0.036	0.036	0.001
B35A0187	41.680	41.948	-0.268	0.268	0.072
B35A0189	42.880	42.746	0.134	0.134	0.018
B35A0191	41.670	41.813	-0.143	0.143	0.020
B35A0192	41.660	41.784	-0.124	0.124	0.015
B35A0194	45.610	44.564	1.046	1.046	1.094
B35A0196	41.000	41.253	-0.253	0.253	0.064
B35A0197	41.300	41.477	-0.177	0.177	0.031
w061707023	41.500	41.723	-0.223	0.223	0.049
Sum			-0.048	2.405	1.365
Average	42.24	42.25			
Calculated			**ME**	**MAE**	**RMSE**
			-0.005	0.267	0.389

Table 9: Observed and simulated head with calculated error assessment for 9 piezometers (post-2011)

Pre-2011 scenario					
Bore hole ID	Observed head[m]	Simulated head[m]	$(obs - sim)$	$\|obs - sim\|$	$(obs - sim)^2$
B35A0184	42.650	42.382	0.268	0.268	0.0718
B35A0187	41.400	41.870	-0.470	0.470	0.221
B35A0189	42.650	42.500	0.150	0.150	0.022
B35A0191	41.450	41.581	-0.131	0.131	0.017
B35A0192	41.330	41.614	-0.284	0.284	0.081
B35A0194	45.450	45.205	0.245	0.245	0.060
B35A0196	40.980	41.199	-0.219	0.219	0.048
B35A0197	41.100	41.270	-0.170	0.170	0.029
w061707023	40.790	41.293	-0.503	0.503	0.253
Sum					
Average	41.97	42.10			
Calculated			**ME**	**MAE**	**RMSE**
			-0.124	0.271	0.292

Table 10: Observed and simulated head with calculated error assessment for 9 piezometers (pre-2011)

As Tables 9 and 10 show, the difference between the observed heads in the two scenarios was about 27 centimeters. However, the difference between the simulated heads in the two scenarios was about half of it (15 cm). The trend is properly captured by the model, but maybe further calibration could improve the value of this difference.

Table 11 compares the results of the current steady state model with the two models developed by Nyarugwe (2016). The calibration method was same for the former independent models and the current model. The former work in this study area, consist of two phases. In the first attempt, Nyarugwe tried to calibrate the post-2011 period and evaluate the model with the new scenario for pre-2011. However, the results of pre-2011 were not satisfactory, and he decided to take another approach and create the model for only pre-2011. The RMSE in a recent study is 0.292 and 0.389 for the period before and after 2011. In general, the results of former work for each scenario indicate that the current model has more efficient than the previous one. In addition, with this research, one model has been defined for the whole study area which has quite good and reasonable results for two scenarios.

Error metric comparison	**Nyarugwe's models**			**Current model**	
	First model		Second model		
	Pre-2011	Post-2011	Pre-2011	Pre-2011	Post-2011
RMSE [m]	2.401	0.585	0.585	0.292	0.389
MAE [m]	1.558	0.406	0.522	0.271	0.267
ME [m]	-1.269	-0.385	-0.108	-0.124	-0.005

Table 11: Error assessment in compare with previous work

Figure 28 shows the groundwater contour map based on the simulated heads in ModelMuse environment. Since the average discrepancy of the two periods for the simulated heads was about 15 centimeters, the potentiometric maps for both scenarios look very similar. According to the groundwater heads results, the highest heads value located in the west part of the study area and the lowest part extended till the north-east. Therefore, the flow direction is from east and south to the northeast.

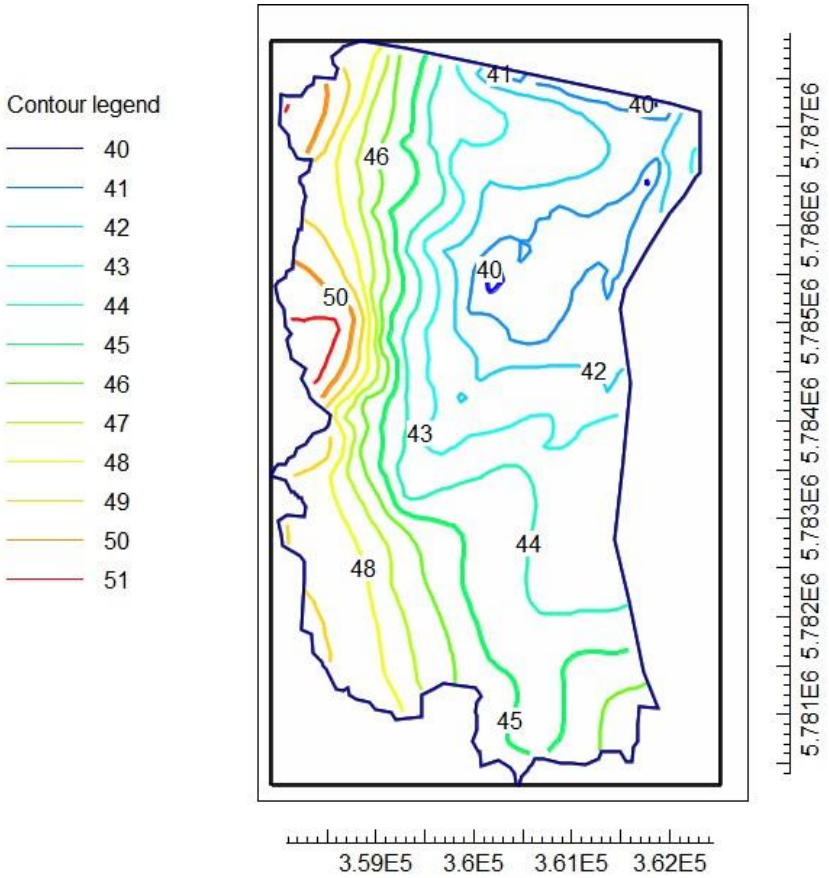

Figure 28: Groundwater contour map [m] for steady state model

4.3.2. Residual

In order to see the bias in the improved steady state model with two scenarios, plotting the residuals versus hydraulic conductivity was done. Figure 29, 30 shows the plot of residual of simulated piezometers heads vs. the observed value. The distributions in these graphs are quite similar. This indicates that the model is not biased. However, as mentioned in previous paragraphs, the piezometer B35A0194 has the most deviation only in one scenario (post-2011). This is the piezometer with the highest head among other piezometers. The piezometer B35A0194 located nearby the upstream of the Glanerbeek creek near to a recreational camp site.

Besides, these plots show that most of the residuals are within ±0.4 meters from the observed heads in the post-2011 and ±0.6 meters in the pre-2011 scenario. These residuals of the Nyarugwe (2016) model were about ±0.6 and ±2 meters for the post- and pre-2011 situations, respectively. In comparison with the Nyarugwe (2016) models, the piezometer B35A0194 still is the outlier with a high residual value, but the current model simulates the observed situation much better. (Figure 30).

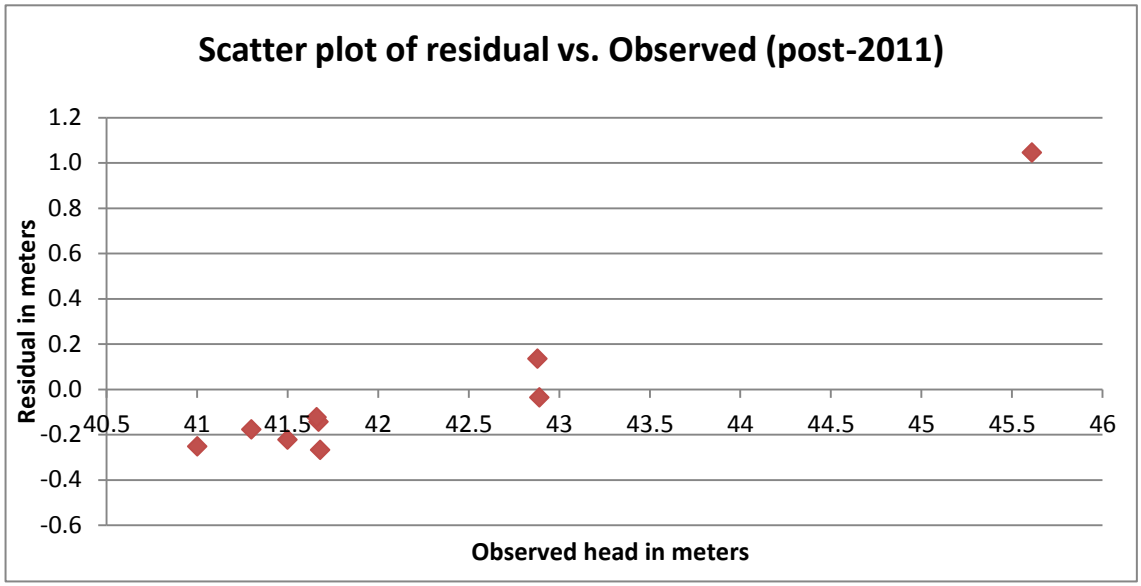

Figure 29: Plot of residual of calibration (post-2011)

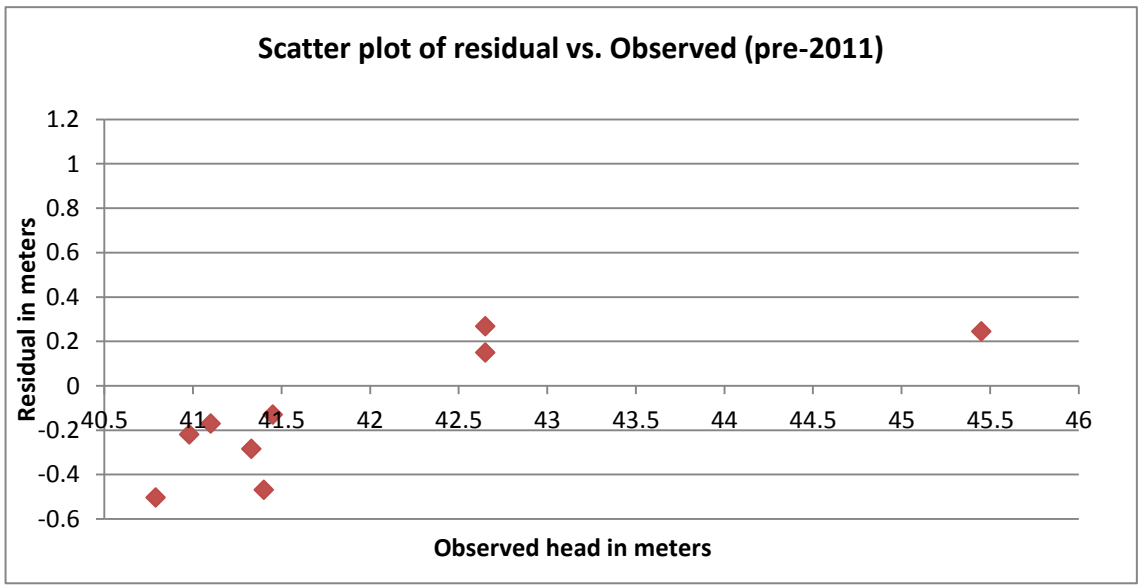

Figure 30: Plot of residual of calibration (pre-2011)

4.3.3. Water balance

The groundwater budget of the model for both scenarios retrieved from the MODFLOW listing file are shown in Tables 12 and 13. These tables show the total daily inflows and outflows from the study area. Recharge, reservoir, and stream leakage were the source of inflow to the model. The outflow components of water balance were drain, evapotranspiration, and stream leakage.

In both periods of interest, the gross recharge constitutes the major part almost 76%. The inflow of gross recharge is 28036 and 28071 m^3d^{-1} in the post and pre-2011 scenarios, respectively. The slight difference in the recharge component between two scenarios refers to the minor different precipitation ($0.001md^{-1}$) as a driving force. The groundwater evapotranspiration also has 1% difference between the two scenarios. This also agrees with the results of the calculated average PET in section 4.1 which indicates that the

average calculated PET in post-2011 is higher than pre-2011. Although the rate of the change in an average evapotranspiration value in different scenarios (4.00E-5) is less than the rate of changes in precipitation (1.00E-3), the impact of that to the model is more tangible in ET package. This could be due to the dissimilar evapotranspiration value distribution by raster file based on the landcover as an input to the model.

1. Water balance for post-2011					
Budget component	Inflow (m^3d^{-1})	*Distribution*	**Budget component**	Outflow (m^3d^{-1})	*Distribution*
Gross Recharge(R_g)	28036	76.7%	Drain	4702	12.86%
Reservoir leakage	247.955	0.67%	GW Evapotranspiration	4927.597	13.47%
Stream leakage	8275.435	22.63%	Stream leakage	26952.9668	73.67%
Total	36559.3908			36583.043	
		IN_OUT	-23.6522		
		Percent Discrepancy	-0.06%		

Table 12: summary of water budget components of the post-2011 period in m^3d^{-1}

2.Water balance for pre-2011					
Budget component	Inflow (m^3d^{-1})	*Distribution*	**Budget component**	Outflow (m^3d^{-1})	*Distribution*
Gross Recharge(R_g)	28071	76.6%	Drain	7467.668	20.35%
Reservoir leakage	267.03	0.72%	GW Evapotranspiration	4595.656	12.52%
Stream leakage	8307	22.68%	Stream leakage	24618.13	67.13%
Total	36645.03			36681.45	
		IN_OUT	-36.423		
		Percent Discrepancy	-0.09%		

Table 13: summary of water budget components of the pre-2011 period in m^3d^{-1}

Hydrological parameter	Pre-2011(2007-2011)	Post-2011(2012-2016)
Average of actual evapotranspiration[md^{-1}]	0.00161	0.00165
Average of precipitation [md^{-1}]	0.021	0.020

Table 14: Average driving forces within the different period time by Twente KNMI data

Reservoir leakage in the whole model has a small proportion which was 0.67% and 0.72 % for pre-2011 and post-2011. The other inflow component in post-2011 was the stream leakage as it has an inflow of

8275 and 8307 and outflow of 26952 and 24618 m^3d^{-1} for post-2011 and pre-2011 to the groundwater, respectively. The minor differences in inflows or outflows were due to the different surface water courses for each scenario. Before the modification, the water was routed into the drain system so that the stream length was less than in post-2011 scenario and this affected the leakage (Figure8). Thus, the out flow of post-2011 has a larger distribution (73%) rather than pre-2011 (67%) out flow. The ratio of inflow to out flow of stream leakage for both scenarios is about $^1/_3$. The discrepancy indicates how much the water budget of entire model close to the water balance. So that, the water budget of the entire model must be within the acceptable range of discrepancy. The final model discrepancy in present study is less than 0.1% for each scenario; therefore, the model meets the discrepancy limitation. Figure 31 and Figure 32 are shown the schematic of water budget component in two different scenarios.

One of the other water budget components for outflow is drain. The drain contribution percent before the modification was 20% in which the tube drained the 7467m^3d^{-1} amount of water out of the study area. By blocking the drain tube, the amount of water that routed out of the system decreased (4702 m^3d^{-1}).

The term "validation" between groundwater modelers and nonmodeler has a different meaning. In nonmodelers perspective, models should capable of making accurate forecast; however, the truth cannot be demonstrated in any model of the natural world (Anderson et al., 2015). The calibrated steady state models in groundwater could only be validate in a limited extent. Despite this fact, this model can be validated (to certain extend) with river discharge data because those are independent data from groundwater observations. The discharge values were available only for the period after 2012, with a rough estimate of 21500m^3d^{-1} (the water authority warned that the discharge data has limited accuracy due to measurement difficulties). This value was used to evaluate the model (3.3.10). The discharge output of the model simulation derived about 19880m^3d^{-1} which is a quite good correspondence.

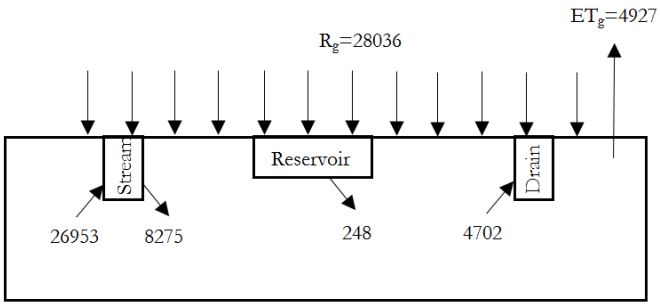

Figure 31: Schematic representation of volumetric Water budget for post-2011 (all units are in md^{-1})

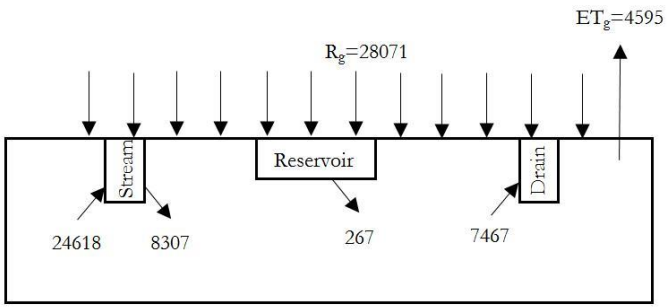

Figure 32: Schematic representation of volumetric Water budget for pre-2011 (all units are in md^{-1})

4.1. Sensitivity analysis

In order to assess the response of the model to changes of certain parameters, a sensitivity analysis was carried out. The tested parameters in this steady state model are horizontal and vertical hydraulic conductivity, stream depth, drain depth and drain conductance. Regarding the fact that the streambed conductance is depended on the horizontal hydraulic conductivity, the sensitivity analysis for streambed conductance has not been performed separately.

Figure 33 shows the comparison of model responses to changing the horizontal hydraulic conductivity and vertical hydraulic conductivity values. The results show that the model is more sensitive to the horizontal hydraulic conductivity rather than the vertical hydraulic conductivity. For the horizontal hydraulic conductivity, the model response is higher to a higher value and lower to a lower value. For the vertical hydraulic conductivity, model responds to both higher and lower values although the sensitivity is negligible. Tables shows the different RMSE values by changing the parameter.

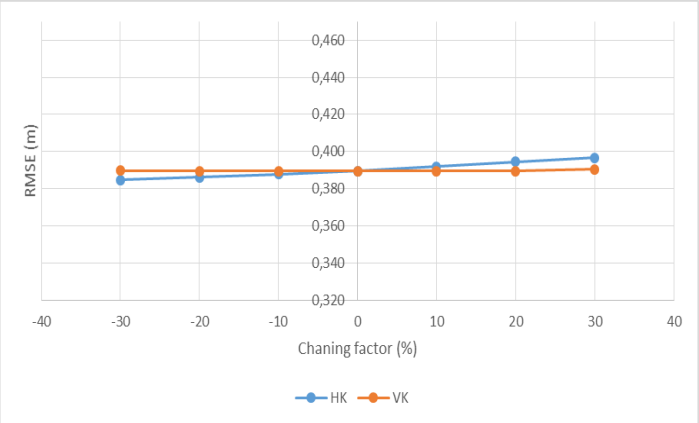

Figure 33: sensitivity analysis of model for horizontal and vertical hydraulic conductivity

Changing factor	Horizontal hydraulic conductivity (HK)	Vertical hydraulic conductivity (VK)
-30 %	0,385	0,390
-20 %	0,386	0,389
-10 %	0,388	0,389
0	0,389	0,389
10 %	0,392	0,389
20 %	0,394	0,389
30 %	0,397	0,390

The result of sensitivity analysis for the drain depth and the drain conductance in the pre-2011 scenario is shown in figure 34. This figure show that the influence of changing the drain depth on simulated heads is considerable and the model responds highly to both increasing and decreasing the drain depth. For the drain conductance, the result shows that RMSE rises by increasing the drain conductance values and decreases by reducing the values; however, the variation is not significant and model responses to the drain conductance is negligible.

To sum up, in pre-2011 scenario, model is more sensitive to the drain depth rather than to the drain conductance.

Figure 35 presents the result of sensitivity analysis for the drain depth and the drain conductance in the post-2011 scenario. According to this figure, the model is more sensitive to the higher values of the drain depth and by increasing the values, RMSE is also increasing. Moreover, decreasing the drain depth resulted in declining the RMSE. For the drain conductance, changing the conductance values have small effect on the RMSE values between observed and simulated heads.

Lastly, for the post-2011 scenario also, the model is more sensitive to the drain depth rather than to the drain conductance. Moreover, comparing the results of sensitivity analysis for the drain depth in pre-2011 and post-2011 scenarios, the model sensitivity is higher to the drain depth in pre-2011 scenario rather than post-2011 scenario.

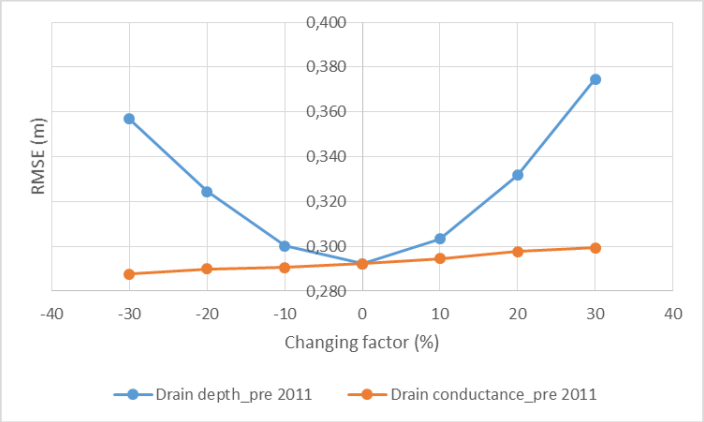

Changing factor	Drain depth pre-2011	Drain conductance pre-2011
-30 %	0,357	0,288
-20 %	0,324	0,290
-10 %	0,300	0,291
0	0,292	0,292
10 %	0,303	0,295
20 %	0,332	0,298
30 %	0,375	0,299

Figure 34: sensitivity analysis of model for the drain depth and drain conductance in pre-2011 scenario.

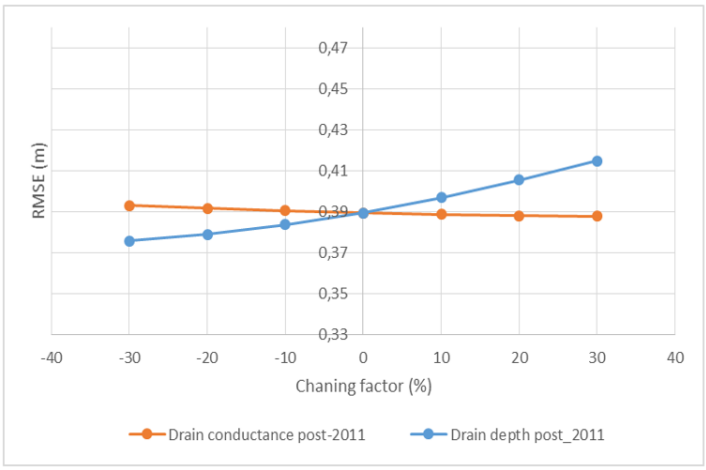

Changing factor	Drain depth post_2011	Drain conductance post-2011
-30 %	0,376	0,393
-20 %	0,379	0,392
-10 %	0,384	0,391
0	0,389	0,389
10 %	0,397	0,389
20 %	0,406	0,388
30 %	0,415	0,388

Figure 35: sensitivity analysis of model for the drain depth and drain conductance in post-2011 scenario.

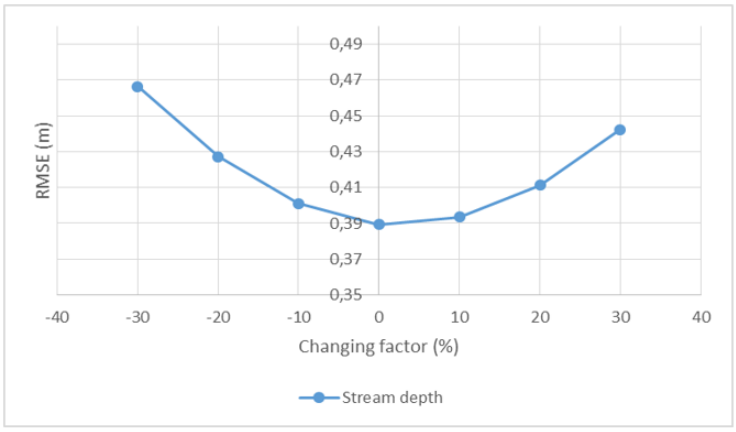

Changing factor	Stream depth
-30 %	0,466
-20 %	0,427
-10 %	0,401
0	0,389
10 %	0,394
20 %	0,411
30 %	0,442

Figure 36: sensitivity analysis of model for the stream depth

Figure 36 shows the result of sensitivity analysis for the stream depth in the post-2011 scenario and it represents that the model is highly sensitive to both higher and lower values of stream depth and by changing the values, RMSE is increasing.

In summary, the model responses to the change of the selected parameters are shown in figure 37. By comparing the responses to the parameters, the most sensitive parameters are the stream depth and drain depth while the vertical hydraulic conductivity and drain conductance are hardly shown responses. However, the model is more sensitive in the drain depth which is in the model set up of pre-2011 rather than the total drain depth in the model.

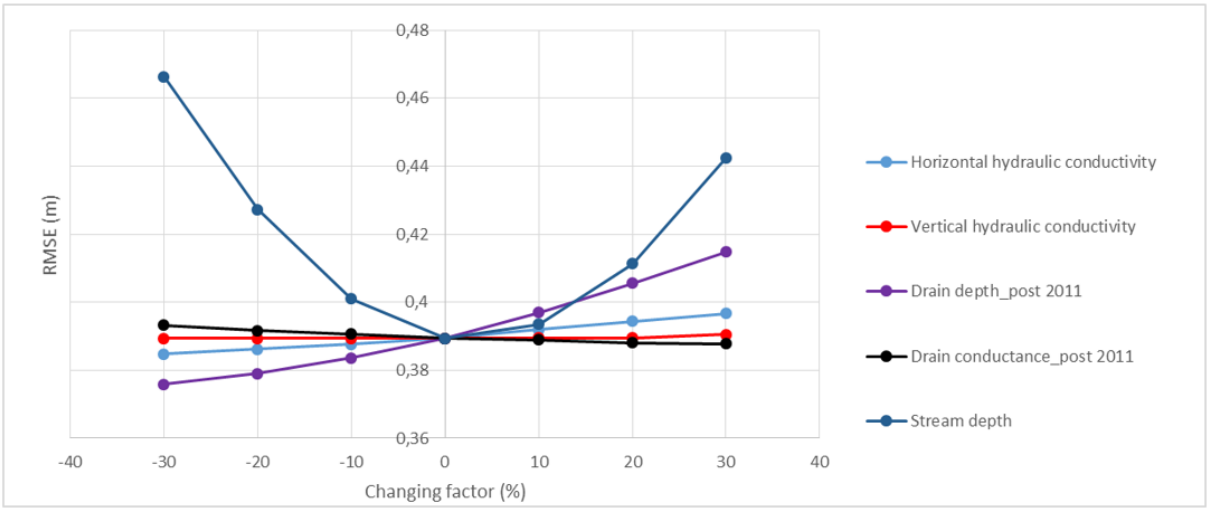

Figure 37: Comparison of model response for selected parameters (such as: horizontal and vertical hydraulic conductivity, stream depth, drain depth and drain conductance).

5. CONCLUSION AND RECOMMENDATION

5.1. Conclusion

The main objective of this study was to create a groundwater model which is able to simulate the hydrology of the Aamsveen in two scenarios, which represent the effects of the hydraulic interventions executed in 2011 for reconstructing the historic wetland circumstances. The pre-2011 scenario represent the situation in 20117-2011, whilst the post-2011 scenario represents the situation in the wetland in the period of 2011-2015.

This work builds upon a similar modeling attempt by Nyarugwe (2016) using MODFLOW-2005 in the ModelMuse environment. The here-reported steady state model was developed using MODFLOW-NWT in the ModelMuse environment. Trial and error method was used for calibration using groundwater levels in selected piezometers as calibration targets. Results of the steady-state calibration in both scenarios are meeting the calibration targets, demonstrated with the squared correlation coefficient (R^2) of 0.979 for pre-2011 and 0.989 for the post-2011 scenario.

The accuracy of the modeling depends very much on certain parameters and how well they are defined. Driving forces such as potential evapotranspiration and precipitation are spatially variable and highly depend on the land cover; therefore, a land cover map was created from a Sentinel-2A image with the 7 most important land cover classes. The overall accuracy of the classification was 96%. Based on this map, the spatial distributions of four parameters were defined for both scenarios, i.e., the K_c factor, the EXTD, the PET, the interception and the infiltration rate has been defined for each scenario.

Moreover, with direct measurements and observation during a field work, initial hydraulic conductivity values and hydraulic conductivity zones calculated from the texture data of the Dutch bational soil database were validated. The hydraulic conductivity values were selected in a one order of measurement magnitude with the range of 0.07 to 2.3 md^{-1} for the peat layer and 2.4 to 25 md^{-1} for the sand layer.

Returning to the question posed at the beginning of the study, it is now possible to state that the water balance components of the model are as following: In the post-2011 scenario, gross recharge contributed 76.7% of total inflow to the aquifer system, stream leakage has 22.6%, and the remaining part, which is less than one percent was covered by reservoir leakage. The main outflows of the aquifer system in this scenario were stream leakage, evapotranspiration and drain with 73.6%, 13.5%, and 12.8% contributions.

Moreover in the pre-2011 scenario, also gross recharge is the major inflow to the groundwater system with 76.6%. The 22.68% goes to stream and the remaining part, similarly to the post-2011 scenario, covered by reservoir leakage. The major part of outflow component is stream leakage in this scenario which is 67%. Drain and evapotranspiration have 20% and 12% contribution in the groundwater outflows, respectively.

Comparison of the water budgets of the two scenarios confirmed the aim of the hydraulic water management interactions in 2011. In this sense, we can conclude that the changes in the surface water courses affected to the water balance of the Aamsveen in the desired direction. It is not easy to validate the model since very limited measured flow data existes and the existing ones are of limited reliability. Nevertheless, the simulated discharges of the rivers in the model in the post-2011 scenario are different from the measured discharges only by about 10%.

The average of the observed hydraulic heads in the post-2011 scenario is more than the average of observed heads in pre-2011 scenario by +26 centimetres. The model simulation also shows the correct trend but somewhat smaller value: +14 centimetres.
The sensitivity analysis was carried out by evaluating the sensitivity of the model to the changes of selected parameters, such as the horizontal and vertical hydraulic conductivities, drain depth, stream depth, and drain conductance. The analysis shows that the model is very sensitive to the stream depth and drain depth. Moreover, the model responses to the vertical hydraulic conductivity and drain conductance would be negligible. Considering the part of drain tube which was located inside the wetland in pre-2011, another analysis shows that the model is sensitive to the proper modeling of the depth of this drain section.
In summary, the present simulation model with the two scenarios shows reasonable water balance closure and low RMSE value between simulated and observed heads. In this research, by fine tuning the conductivities, the geometry of the model, and assigning a detailed potential evapotranspiration map the model represents a good simulation of the Aamsveen wetland's hydraulic system. This model is a promising starting point for the future research in this area.

5.2. Recommendations

- The present model used the model top layer which was used in regional model from iMod. In this DEM file, the elevations on the Dutch and German sides of the boarder do not match properly. Further studies should choose a better digital elevation model since the shallow aquifer makes this model very sensitive to errors in the representation of the surface.
- The spatial variability in potential evapotranspiration has been considered in this model. In other word, the land cover map was created based on the current situation by satellite for two scenarios. It would be better if the temporal variability of the land use map would be taken into account.
- ZONEBUDGET can calculate the sub-regional water budget by using the results from MODFLOW simulation. Hence, in order to get a mere detailed understanding of the water budget in the wetland, the use of ZONEBUDGET is recommended.
- The simulation of some fluxes which are interacting between the surface and the groundwater (such as recharge, groundwater evapotranspiration and groundwater exfiltration) could be more realistically simulated by applying the UZF package through MODFLOW_NWT. UZF package simulates the process much better than the here-applied evapotranspiration package and therefore, it is recommended for the further studies in groundwater and surface water interaction.
- In reality, a number of the parameters are time-dependent and it can influence the model results. Moreover, transient fluxes are more reliable than steady-state fluxes and thus, a transient approach is highly recommended for the future studies.

LIST OF REFERENCES

Allen, R. G., Pereira, L. S., Raes, D., Smith, M., & Ab, W. (1998). Crop evapotranspiration-Guidelines for computing crop water requirements-FAO Irrigation and drainage paper 56, 1–15. http://doi.org/https://doi.org/10.1016/j.eja.2010.12.001

Anderson, M. P., Woessner, W. W., & Hunt, R. J. (2015). *Applied groundwater modeling : simulation of flow and advective transport* (2). San Diego: Elsevier Science.

Andriesse, J. P. (1988). *Nature and management of tropical peat soils_FAO SOILS BULLETIN 59*. Rome, Italy: Food and Agriculture Organization of the United Nations.

Armandine Les Landes, A., Aquilina, L., De Ridder, J., Longuevergne, L., Pagé, C., & Goderniaux, P. (2014). Investigating the respective impacts of groundwater exploitation and climate change on wetland extension over 150 years. *Journal of Hydrology*, *509*, 367–378. http://doi.org/10.1016/j.jhydrol.2013.11.039

Bakker, W. H., Feringa, W., Gieske, A. S. M., Gorte, B. G. H., Grabmaier, K. A., Hecker, C. A., … Westinga, E. (2001). *Principles of Remote Remote Sensing - An introductory text book*. (K. Tempfli, N. Kerle, G. C. Huuneman, & L. L. F. Jansen, Eds.). The International Institute for Geo-Information Science and Earth Observation (ITC),.

Banta, E. R. (2000). MODFLOW-2000, The U.S. Geological Survey Modular Ground-Water Model-Documentation of Packages for Simulating Evapotranspiration with a Segmented Function (ETS1) and Drains with Return Flow (DRT1). Open-File Report 00-466. Retrieved April 12, 2017, from http://water.usgs.gov/nrp/gwsoftware/modflow2000/ofr00-466.pdf

Bell, J.S. & van 't Hullenaar, J. W. (2015). *Ecohydrologische systeemanalyse dal van de Glanerbeek*. Zwolle.

Best, E. P. H., Verhoeven, J. T. A., & Wolff, W. J. (1993). The ecology of The Netherlands wetlands: characteristics, threats, prospects and perspectives for ecological research. *Hydrobiologia*, *265*(1-3), 305–320. http://doi.org/10.1007/BF00007274

Brown, L. E., Mitchell, G., Holden, J., Folkard, A., Wright, N., Beharry-Borg, N., … Woulds, C. (2010). Priority water research questions as determined by UK practitioners and policy makers. *Science of the Total Environment*, *409*(2), 256–266. http://doi.org/10.1016/j.scitotenv.2010.09.040

Campbell, G. S. (1995). *SOIL PHYSICS WTTH BASIC , Transport Models for Soil_Plant Systems*. Washington, D.C.: Department of Agronomy and Soils, Washington State University, Pullman U.S.A.

Corbett, E. S., & Crouse, R. P. (1997). Rainfall interception by a. *Science*, *199*, 346–359.

Dufour, F. C. (2000). Groundwater in Netherland: facts and figures. *Netherlands Institude of Applied Geoscience TNO (Delft)*, 96 PP.

Educational, U. N. (1971). MULTILATERAL Convention on wetlands of international importance espe cially as waterfowl habitat . Concluded at Ramsar , Iran , on 2 February 1971 Authentic texts : English , French , German and Russian . Convention relative aux zones humides d ' importan, *996*(14583).

Fleming, M., & Neary, V. (2004a). Continuous Hydrologic Modeling Study with the Hydrologic Modeling System. *Journal of Hydrologic Engineering*, *9*(3), 175–183. http://doi.org/10.1061/(ASCE)1084-0699(2004)9:3(175)

Fleming, M., & Neary, V. (2004b). Continuous Hydrologic Modeling Study with the Hydrologic Modeling System. *Journal of Hydrologic Engineering*, *9*(3), 175–183. http://doi.org/10.1061/(ASCE)1084-0699(2004)9:3(175)

Ghimire, C. P., Bruijnzeel, L. A., Lubczynski, M. W., & Bonell, M. (2012). Rainfall interception by natural and planted forests in the Middle Mountains of Central Nepal. *Journal of Hydrology*, *475*, 270–280. http://doi.org/10.1016/j.jhydrol.2012.09.051

Hiemstra, P., & Sluiter, R. (2011). *Interpolation of Makkink evaporation in the Netherlands*. Retrieved from http://www.numbertheory.nl/files/report_evap.pdf

Hill, M. (1998). Methods and guidelines for effective model calibration: US Geological Survey Water-Resources Investigations Report 98-4005, 90 p. *US Geological Survey,Water Resources Investigations Report 98-4005*, 1–98. Retrieved from from https://water.usgs.gov/nrp/gwsoftware/modflow2000/WRIR98-4005.pdf

Kinzelbach, W. (1986). Groundwater modeling: An Introduction with Samples programs in BASIC. ELSEVIER SCIENCE . http://doi.org/10.1016/S0167-5648(08)70745-7

KNMI. (2016). Retrieved August 15, 2016, from https://www.knmi.nl/nederland-

nu/klimatologie/uurgegevens
Kresic, N. (2007). *Hydrogeology and Groundwater Modeling* (2nd ed.). Bosa Roca: CRC Press.
Kuhry, P. (1985). Transgression of a raised bog across a coversand ridge originally covered with an oak-lime forest. Palaeoecological study of a Middle Holocene local vegetational succession in the Amtsven (northwest Germany). *Review of Palaeobotany and Palynology*, *44*(3-4). http://doi.org/10.1016/0034-6667(85)90023-5
Landschap Overijssel, N. (2007). *Natura 2000-gebied 55 - Aamsveen*.
Leuning, R., Condon, A. G., Dunin, F. X., Zegelin, S., & Denmead, O. T. (1994). Rainfall interception and evaporation from soil below a wheat canopy. *Agricultural and Forest Meteorology*, *67*(3-4), 221–238. http://doi.org/10.1016/0168-1923(94)90004-3
Lubczynski, M. W., & Gurwin, J. (2005). Integration of various data sources for transient groundwater modeling with spatio-temporally variable fluxes - Sardon study case, Spain. *Journal of Hydrology*, *306*(1-4), 71–96. http://doi.org/10.1016/j.jhydrol.2004.08.038
Malekmohammadi, B., & Rahimi Blouchi, L. (2014). Ecological risk assessment of wetland ecosystems using Multi Criteria Decision Making and Geographic Information System. *Ecological Indicators*, *41*, 133–144. http://doi.org/10.1016/j.ecolind.2014.01.038
McElwee, C. D. (1987). Sensitivity Analysis of Ground-Water Models. In *Advances in Transport Phenomena in Porous Media* (pp. 751–817). Dordrecht: Springer Netherlands. http://doi.org/10.1007/978-94-009-3625-6_17
McMahon, T. A., Peel, M. C., Lowe, L., Srikanthan, R., & McVicar, T. R. (2013). Estimating actual, potential, reference crop and pan evaporation using standard meteorological data: a pragmatic synthesis. *Hydrology and Earth System Sciences*, *17*(4), 1331–1363. http://doi.org/10.5194/hess-17-1331-2013
Mishra, H. S., Rathore, T. R., & Pant, R. C. (1997). Root growth, water potential, and yield of irrigated rice. *Irrigation Science*, *17*, 69–75. http://doi.org/10.1007/s002710050024
Naiman, R. J., Magnuson, J. J., McKnight, D. M., & Stanford, J. A. (2013). *The Freshwater Imperative: A Research Agenda*. Washington, D.C.: Island Press.
Natura 2000 Networking Programme. (2007). Retrieved March 1, 2017, from http://www.natura.org/about.html
Niswonger, B. R. G., & Prudic, D. E. (2005). Documentation of the Streamflow-Routing (SFR2) Package to Include Unsaturated Flow Beneath Streams — A Modification to SFR1:U.S. Geological Survey Techniques and Methods 6-A13. In US Geological Survey Techniques and Methods 6 (p. 50).
Niswonger, R. G., Panday, S., & Ibaraki, M. (2011). MODFLOW-NWT , A Newton Formulation for MODFLOW-2005. *U.S. Geological Survey Techniques and Methods 6-A37*, 44.
Niswonger, R. G., Prudic, D. E., & Regan, S. R. (2006). Documentation of the Unsaturated-Zone Flow (UZF1) Package for Modeling Unsaturated Flow Between the Land Surface and the Water Table with MODFLOW-2005. *Book 6, Modeliing Techniques, Section A, Ground Water*, 71.
Nyarugwe, K. P. (2016). *Effect of surface water management measures on a groundwater fed wetland. MSc Thesis*. University of Twente Faculty of Geo-Information and Earth Observation (ITC). Retrieved from http://www.itc.nl/library/papers_2016/msc/wrem/nyarugwe.pdf
Pellenbarg, N. P. (1989). *Groundwater management in the Netherlands: Background and legislation groundwater in the Netherlands. Groundwater Management: Sharing responsibility for an open access resource*. Wageningen, Netherlands.
Prudic, D. E., Konikow, L. F., & Banta, E. R. (2004). *To Simulate Stream-Aquifer Interaction With Modflow-2000 Streamflow-Routing. America*.
Shah, N., Nachabe, M., & Ross, M. (2007). Extinction depth and evapotranspiration from ground water under selected land covers. *Ground Water*, *45*(3), 329–38. http://doi.org/10.1111/j.1745-6584.2007.00302.x
Simmons, K., Deatric, J., & Levis, B. (2014). *Soil Sampling. Us Epa*.
Teketel, A. T. (2017). INTEGRATED HYDROLOGICAL MODELING OF SURFACE - GROUNDWATER INTERACTIONS The case of Denpasar-Tabanan Basin in the Southern Bali Island. *MSc Thesis*.
Van Der Meulen, M. J., Doornenbal, J. C., Gunnink, J. L., Stafleu, J., Schokker, J., Vernes, R. W., … Van Daalen, T. M. (2013). 3D geology in a 2D country: Perspectives for geological surveying in the Netherlands. *Geologie En Mijnbouw/Netherlands Journal of Geosciences*, *92*(4), 217–241. http://doi.org/10.1017/S0016774600000184
van Dijk, A. I. J. ., & Bruijnzeel, L. . (2001). Modelling rainfall interception by vegetation of variable

density using an adapted analytical model. Part 1. Model description. *Journal of Hydrology*, *247*(3), 230–238. http://doi.org/10.1016/S0022-1694(01)00392-4

Vend, V. de. (1986). *Man-made lowlands : history of water management and land reclamation in the Netherlands*. Utrecht: Uitgeverij Matrijs. Retrieved from https://secure.matrijs.com/Man-made-lowlands.-History-of-water-management-and-land-reclamation-in-the-Netherlands.html

Wang, G., Wang, D., & Anagnostou, E. N. (2007). Evaluation of canopy interception schemes in land surface models. *Journal of Hydrology*, *347*(3-4), 308–318. http://doi.org/10.1016/j.jhydrol.2007.09.041

Wang, Y. L., Wang, X., Zheng, Q. Y., Li, C. H., & Guo, X. J. (2012). A Comparative Study on Hourly Real Evapotranspiration and Potential Evapotranspiration during Different Vegetation Growth Stages in the Zoige Wetland. *Procedia Environmental Sciences*, *13*(2011), 1585–1594. http://doi.org/10.1016/j.proenv.2012.01.150

Weldemichiel, M. Y. (2015). *Integrated numerical modeling of hard- rock aquifers applying stratiform conceptual model in Sardon catchment study case , Spain*. *MSc Thesis*. University of Twente Faculty of Geo-Information and Earth Observation (ITC). Retrieved from http://www.itc.nl/library/papers_2016/msc/wrem/weldemichael.pdf

Wetlands International. (2015). Retrieved from https://www.wetlands.org/the-problem/what-are-wetlands/

Wikipedia. (2016). Retrieved January 30, 2015, from https://nl.wikipedia.org/wiki/Aamsveen

Wong, T., Batjes, D., & Jager, J. de. (2007). *Geology of the Netherlands*. Hardbound: Royal Netherlands Academy of Arts and Sciences.

Wu, J., & Zeng, X. (2013). Review of the uncertainty analysis of groundwater numerical simulation. *Chinese Science Bulletin*, *58*(25), 3044–3052. http://doi.org/10.1007/s11434-013-5950-8

Xing, L. (2015). *Wetland reconstruction by controlling water level in Aamsveen : the effects on variation of vegetation and nutrients Wetland reconstruction by controlling water level in Aamsveen : the effects on variation of vegetation and*. *MSc Thesis*. University of Twente Faculty of Geo-Information and Earth Observation (ITC). Retrieved from http://www.itc.nl/library/papers_2015/msc/wrem/xing.pdf

Xu, C.-Y., & Singh, V. P. (2002). Cross Comparison of Empirical Equations for Calculating Potential Evapotranspiration with Data from Switzerland. *Water Resources Management*, *16*(3), 197–219. http://doi.org/10.1023/A:1020282515975

Zehairy, A. El. (2014). *Assessment of lake-groundwater interactions - Turawa Case, Poland*. *MSc Thesis*. University of Twente Faculty of Geo-Information and Earth Observation (ITC). Retrieved from http://www.itc.nl/library/papers_2014/msc/wrem/zehairy.pdf

Appendix

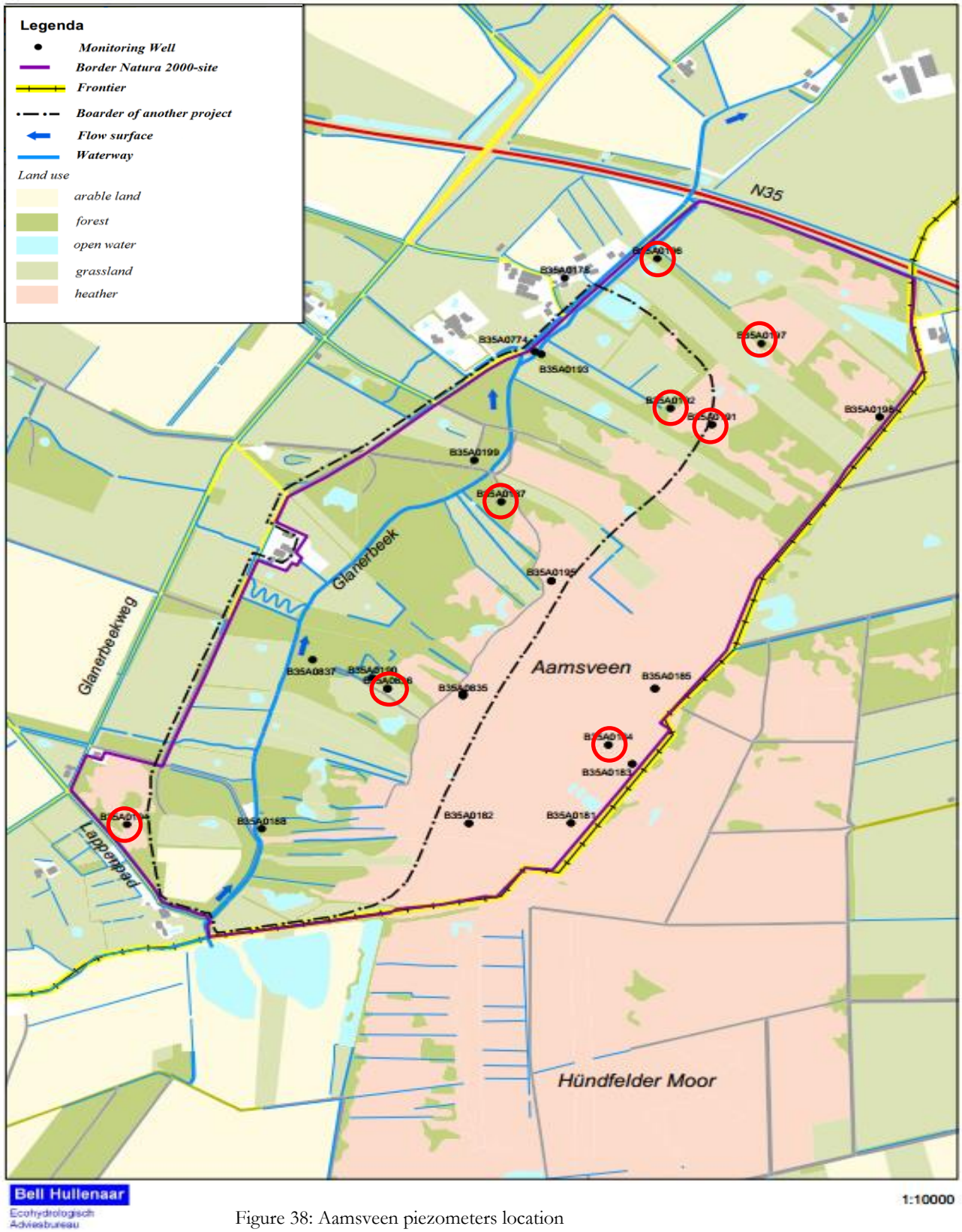

Figure 38: Aamsveen piezometers location

Appendix 2

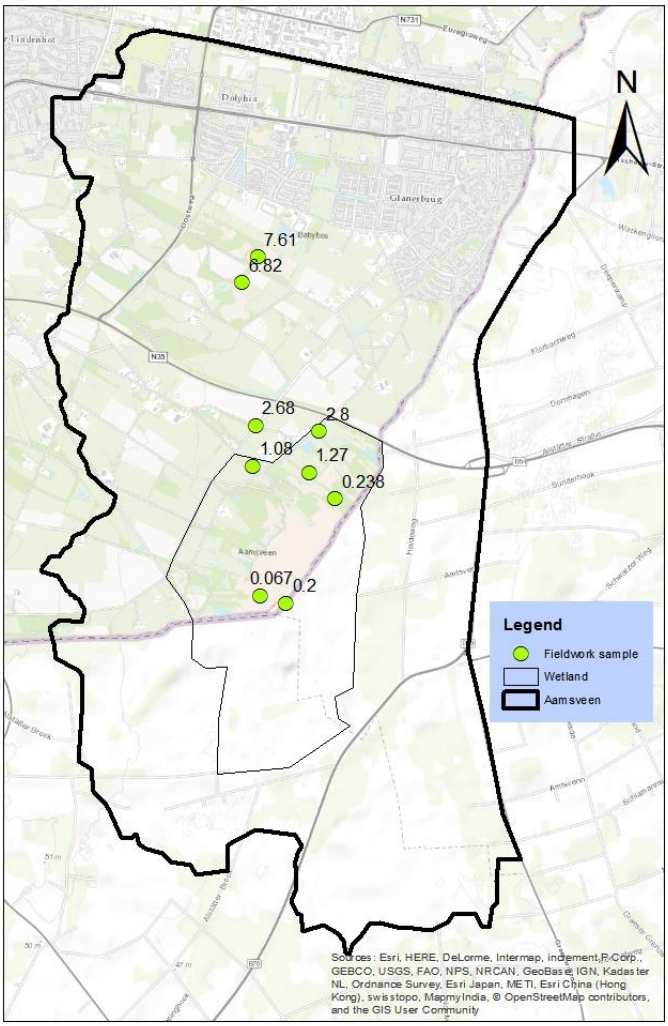

Figure 39: Fieldwork samples distribution

Appendix 3

Laboratory method using Permeameter

In this method, the samples have been put in the container of the Permeameter; and the siphons which were filled with water, have been placed in the ring holder and connected to the numbered synthetic pipes. When the water table above the ring holder falls and being equal to the siphon level, drained off water flows to the pipe and since the pipe is filled, water flows into the burette. When the rate of flow to the burette reached the stationary value, equation 1 in the text can be used to estimate the permeability coefficient.